Thesis

CHARACTERISATION OF RETROGRADE BLOOD-FLOW IN THE MAIN PULMONARY ARTERY IN PATIENTS WITH ELEVATED MEAN PULMONARY ARTERIAL PRESSURE THROUGH CARDIAC MAGNETIC RESONANCE PHASE-CONTRAST IMAGING

A RETROSPECTIVE STUDY

submitted by

Christoph Martin Janig, B.rer.nat.

submitted in partial fulfilment

of the requirements for the degree of

Doctor of Medicine

(Dr. med. univ.)

at the

Medical University of Graz

carried out at the

Division of General Radiological Diagnostics

under guidance of

DI Dr. Ursula Reiter

Univ.-Prof. Dr. Michael Fuchsjäger

Graz, 13.10.2015

Eidesstattliche Erklärung

Ich erkläre ehrenwörtlich, dass ich die vorliegende Arbeit selbstständig und ohne fremde Hilfe verfasst habe, andere als die angegebenen Quellen nicht verwendet habe und die den benutzten Quellen wörtlich oder inhaltlich entnommenen Stellen als solche kenntlich gemacht habe.

Graz, am 13.10.2015 Christoph Martin Janig, eh

Preface

During my medical studies and given my interest in the field of radiology and fascination with MRI, I found Dr. Ursula Reiter as a dedicated advisor and guide through the topic of magnetic resonance phase contrast imaging in pulmonary hypertension. The hours in front of the work stations outlining one region of interest after another, extracting the data, processing it and interpreting it, finally paid off in the form of this thesis and a winning presentation at the International Student Congress of (bio)Medical Sciences 2015, Groningen, Netherlands.

It has been a wonderful journey side by side in front of the screens with this wonderful team.

Acknowledgement

I would like to express my gratitude to Prof. Dr. Michael Fuchsjäger for giving me the opportunity to work in his division of General Radiological Diagnostics for my thesis.

I would also like to thank DI Dr. Ursula Reiter and DI Dr. Gert Reiter who supported me tremendously throughout the whole process of this thesis, without them this would not have been possible.

I would like to thank my family, especially my parents Gerda Janig and Prof. Dr. Herbert Janig with all my heart for their support in my studies and spiritual guidance.

Finally, I would like to thank my girlfriend, Antonia Mühlthaler for her friendship and support.

Table of Contents

Glossary and Abbreviations

AUC	area under the curve
CI	cardiac index
CMRI	cardiac magnetic resonance imaging
CTEPH	chronic thromboembolic pulmonary hypertension
dBP	diastolic blood pressure
dPAP	diastolic pulmonary artery pressure
esp.	especially
HMV	heart minute volume
mmHg	millimetres of Mercury
MPA	main pulmonary artery
mPAP	mean pulmonary artery pressure
MR	magnetic resonance
MRI	magnetic resonance imaging
MR-PCI	magnetic resonance phase contrast imaging
MRT	magnetic resonance tomography
ms	milliseconds
nc	no change
PA	pulmonary artery
PAH	pulmonary arterial hypertension
PAWP	pulmonary wedge pressure
PE	pulmonary embolism
PH	pulmonary hypertension
POPH	portopulmonary hypertension
PPHN	persistent pulmonary hypertension of the newborn
PVR	pulmonary vascular resistance
PWV	pulse wave velocity
RAP	right atrial pressure
rel.	relative
RHC	right heart catheterisation
ROC	receiver operator characteristics
ROI	region of interest
ROT	retrograde flow onset time
rROT	relative retrograde flow onset time
sBP	systolic blood pressure

SD	standard deviation
sPAP	systolic pulmonary artery pressure
SSRI	selective serotonin re-uptake inhibitors
Δ	delta; difference

List of Figures

List of Tables

Zusammenfassung

Pulmonale Hypertonie (PH) ist eine lebensbedrohliche Erkrankung, die bei einer chronischen Erhöhung des pulmonal-arteriellen Mitteldrucks (mPAP) in Ruhe ≥ 25 mmHg leitlinienkonform mittels Rechtsherzkatheter diagnostiziert wird. Magnetresonanz-Phasenkontrastbildgebung (MR-PCI) des Herzens erlaubt erhöhten mPAP aus der Dauer eines charakteristischen Blutflusswirbels im pulmonalen Hauptstamm (MPA) mit physikalischer Genauigkeit abzuschätzen. Diese Wirbelströmung verursacht einen retrograden Blutfluss, dessen Start-Zeit („retrograde flow onset time“ ROT) im Herzintervall als nicht-invasiver Index zur Diagnose von pulmonal-arteriellem Lungenhochdruck (PAH) verwendet werden kann. Das Ziel dieser Studie ist es herauszufinden in wie weit sich diese Methode für alle PH Gruppen verallgemeinern lässt.

In die vorliegende retrospektive Studie wurden 108 Patientinnen/Patienten (n = 54 mit mPAP ≥ 25 mmHg / n = 54 mit mPAP < 25 mmHg), die im Rahmen der Abklärung von PH mit Rechtsherzkatheter untersucht wurden und zeitnah (11±19 Tage) zu einer Herz-Magnetresonanzuntersuchung mit MR-PCI der MPA zugewiesen wurden, eingeschlossen. Gesamtfluss und retrograder Blutfluss in der MPA wurden mittels Routine-Software manuell ausgewertet. Als ROT wurde die Zeitdifferenz zwischen dem Startzeitpunkt des MPA Blutflusses und dem retrograden Fluss definiert. Die Startzeiten wurden dabei mit verschiedenen Fit-Methoden bestimmt. Die statistische Analyse der ROT umfasste Vergleich mittels 2-Stichproben t-Test (Patientinnen/Patienten mit normalem mPAP mit PAH und mit non-PAH-PH), Korrelationsanalyse und Receiver-Operating-Characteristic (ROC) Kurvenanalyse.

Mit der Upslope-Fit Methode konnte ROT in allen Patienten ohne größere Limitationen bestimmt werden. In Patientinnen/Patienten mit PH waren die mittleren ROT signifikant kürzer als in Patientinnen/Patienten mit normalem mPAP (PH: 144±53 ms; non-PH: 271±65 ms; $p < 0.0001$). ROT in PAH und non-PAH-PH unterschied sich nicht signifikant ($p = 0.41$). ROT aller Patientinnen/Patienten korrelierte nur moderat mit dem mPAP ($r = -0.67$). Die ROC-Kurvenanalyse ergab nicht nur für PAH eine hohe diagnostische Genauigkeit (AUC, 0.95; cut-off, 195 ms; Sensitivität/Spezifität, 0.88/0.89) sondern auch allgemein für PH (AUC, 0.94; cut-off, 195 ms; Sensitivität/Spezifität, 0.87/0.89).

Die Ergebnisse der Studie zeigen, dass ROT in der MPA aus MR-PCI der MPA mittels Routine Auswertesoftware bestimmt werden kann. Wenngleich ROT nicht unmittelbar die nicht-invasive Bestimmung von mPAP erlaubt, gelingt die Diagnose mPAP ≥ 25 mmHg nicht nur für PAH, sondern allgemein für PH mit hoher Genauigkeit.

Abstract

Pulmonary hypertension (PH) is a life-threatening disease, which is characterised by an elevation of the mean pulmonary artery pressure (mPAP) at rest ≥25mmHg. According to current guidelines, PH is diagnosed by right heart catheterisation (RHC). Magnetic resonance phase-contrast imaging (MR-PCI) enables to estimate elevated mPAP with physical accuracy by the assessment of the persistence of a characteristic blood flow vortex in the main pulmonary artery (MPA). This vortex causes a retrograde flow whose onset time ("retrograde flow onset time", ROT) in the cardiac interval can be used as a non-invasive index to diagnose pulmonary arterial hypertension (PAH). The purpose of this study was to investigate if this method can be employed for the diagnosis of PH in general.

In the present study 108 patients (n=54 with mPAP≥25mmHg / n=54 with mPAP<25mmHg) who underwent RHC due to the clinical suspicion of PH and who underwent cardiac magnetic resonance imaging around the time of RHC (11±19 days) were retrospectively enrolled. Global and retrospective blood flow in the MPA was manually evaluated with routine software. ROT was defined as the time difference between the onset of forward and retrograde flow in the MPA, and was determined by different fitting algorithms. Resulting ROTs were compared by 2 sample t-test (non-PH/PH and PAH/non-PAH PH), and analysed by correlation analysis and Receiver-Operating-Characteristic (ROC) curve analysis.

Evaluation of ROT by upslope-curve fitting was feasible in all patients without mayor limitations. Mean ROT was significantly shorter in patients with PH compared to patients with normal mPAP (PH: 144±53ms; non-PH: 271±65ms; p<0.0001). PAH and non-PAH PH patients did not show significant differences in ROT (p=0.41). In the present study population, ROT correlated moderately with mPAP (r=-0.67). ROC curve analysis revealed high accuracy of ROT for the diagnosis of PAH (PAH: AUC, 0.95; cut-off, 195ms; sensitivity/specificity, 0.88/0.89) and PH (AUC, 0.94; cut-off, 195ms; sensitivity/specificity 0.87/0.89).

In conclusion, ROT in the MPA can be determined with routine software from MR-PCI of the MPA. Even though mPAP could not be determined from ROT, early onset of ROT is characteristic for PH and allows non-invasive diagnosis of mPAP≥25mmHg with high accuracy.

1 Background

1.1 Pulmonary Hypertension

Pulmonary hypertension (PH) is a disease characterised by an elevation of the mean blood pressure in the main pulmonary artery (MPA). According to current guidelines, PH is diagnosed invasively by right heart catheterisation (RHC). The diagnostic criterion for PH is met, if the mean pulmonary artery pressure (mPAP) is ≥ 25 mmHg at rest. Normal mPAP values are 14 ± 3 mmHg, mPAP between 21 and 24 mmHg are assigned as elevated. Patients with elevated mPAP should be closely followed, at least when there is a risk for developing PAH (which, for example, could be due to connective tissue disease or a positive family anamnesis for a heritable form of PH).(1–3)

At early stages, PH patients are often without symptoms at rest. Moreover, symptoms of PH are rather unspecific, but can include increasing exertional dyspnoea, fatigue, syncope and right-sided heart dysfunction.(1,2)

Due to these unspecific symptoms and the low prevalence of PH, most patients are diagnosed late in the course of the disease, when the prognosis is poor. A prevalence of 97 cases per million has been reported in the UK.(2,4–7)

At the World Symposium on Pulmonary Hypertension 2013 in Nice, France, 5 groups of conditions were defined to cause PH depending on aetiology, pathological findings, hemodynamic characteristics, and therapeutic approaches.(8)(see also Table 1).

Pulmonary arterial hypertension (PAH, Group 1): PAH is a rare disease with an incidence of 5-10 cases per million per year and a prevalence of 15-60 cases per million in Europe. Patients with idiopathic PAH and heritable PAH due to specific gene mutations such as BMPR2 or other members of the TGFβ superfamily are classified as Group 1. Drug or toxin induced PAH (for example induced by Aminorex, Fenfluramine, Dexfenfluramine, toxic rapeseed oil, Benfluorex and SSRIs) as well as PAH associated with infectious diseases such as HIV infection or connective

tissue disease are also included. Moreover, patients with portal hypertension, congenital heart disease, veno-occlusive disease (Group 1') and persistent PH of the newborn (PPHN, Group 1'') are also counted in Group 1.(4,8)

PH due to left heart disease (Group 2): Left heart diseases represent the most frequent cause of PH. Left ventricular or valvular diseases may cause an increase in mPAP by the elevation of left atrial pressure (post-capillary PH). Pulmonary vascular resistance remains mainly normal in this clinical group. Group 2 includes aetiologies like heart failure with reduced, as well as preserved, left ventricular ejection fraction, and patients with left heart valvular diseases.(4,8,9)

PH due to chronic lung disease and/or hypoxia (Group 3): Alveolar hypoxia as a result of lung disease is the predominant cause of PH in Group 3. Moreover, PH in patients with chronic bronchiectasis, cystic fibrosis and parenchymal lung disease are included in this group.(8)

Patients with chronic thromboembolic PH (CTEPH, Group 4): The Spanish PH Registry describes an incidence of 0.9 cases per million per year and a prevalence of 3.2 cases per million. CTEPH occurs in about 4% of patients after surviving an acute pulmonary embolism (PE). Nearly 75% of all CTPH patients had an acute PE and nearly 32% of CTPH cases are associated with thrombophilic disorders and about 3% with splenectomy.(4,8,10,11)

PH due to unclear multifactorial mechanisms (Group 5): Clinical Group 5 includes several forms of PH with unclear or multifactorial aetiology. The predominant aetiologies in this group are systemic and hematologic disorders associated with increased risk of developing PH, patients in end stage of renal disease, and patients with tumoral obstruction of proximal pulmonary arteries.(8)

As shown by the REVEAL registry, survival rates of PH significantly differ between the clinical groups.(8,12)

Table 1: Classification of pulmonary hypertension according to the fifth World Symposium on pulmonary hypertension 2013, Nice, France. Table after (8)**.** PAH = pulmonary arterial hypertension, BMPR2 = bone morphogenic protein receptor type 2, ALK-1 = activin-like receptor kinase-1, ENG = endoglin, SMAD9 = mothers against decapentaplegic 9, CAV1 = caveolin-1, KCNK3 = Potassium Channel, Two Pore Domain Subfamily K-Member 3, HIV = human immunodeficiency virus, PH = pulmonary hypertension.

1. Pulmonary arterial hypertension
1.1 Idiopathic PAH
1.2 Heritable PAH
1.2.1 BMPR2
1.2.2 ALK-1, ENG, *SMAD9, CAV1, KCNK3*
1.2.3 Unknown
1.3 Drug and toxin induced
1.4 Associated with:
1.4.1 Connective tissue disease
1.4.2 HIV infection
1.4.3 Portal hypertension
1.4.4 Congenital heart diseases
1.4.5 Schistosomiasis
1’ Pulmonary veno-occlusive disease and/or pulmonary capillary hemangiomatosis
1’’. Persistent pulmonary hypertension of the newborn
2. Pulmonary hypertension due to left heart disease
2.1 Left ventricular systolic dysfunction
2.2 Left ventricular diastolic dysfunction
2.3 Valvular disease
2.4 Congenital/acquired left heart inflow/outflow tract obstruction and congenital cardiomyopathies
3. Pulmonary hypertension due to lung diseases and/or hypoxia
3.1 Chronic obstructive pulmonary disease
3.2 Interstitial lung disease
3.3 Other pulmonary diseases with mixed restrictive and obstructive pattern
3.4 Sleep-disordered breathing
3.5 Alveolar hypoventilation disorders
3.6 Chronic exposure to high altitude
3.7 Developmental lung diseases

Table 1 continued on page 17

Table 1 continued from page 16

4. Chronic thromboembolic pulmonary hypertension (CTEPH)
5. Pulmonary hypertension with unclear multifactorial mechanisms
5.1 Hematologic disorders: chronic haemolytic anaemia, myeloproliferative disorders, splenectomy
5.2 Systemic disorders: sarcoidosis, pulmonary histiocytosis, lymphangioleiomyomatosis
5.3 Metabolic disorders: glycogenstorage disease, Gaucher disease, thyroid disorders
5.4 Others: tumoral obstruction, fibrosing mediastinitis, chronic renal failure, segmental PH

1.2 Right Heart Catheterisation

RHC is the established reference standard to determine right heart and pulmonary pressures and hemodynamic. According to current guidelines for RHC in patients with suspicion for PH, the investigation should include the assessment of pressures in the right atrium, right ventricle, and pulmonary artery, the pulmonary arterial pressure in the "wedge" position (pulmonary arterial wedge pressure (PAWP)), right ventricular cardiac output (CO), and mixed-venous oxygen saturation (to evaluate cardiac left-to-right shunts). Table 2 summarises RHC based hemodynamic normal values and respective pathophysiological alterations in the clinical PH groups.(2)

Table 2: Right heart hemodynamic parameters typically assessed by right heart catheterisation (RHC). Table after (13)**.** mPAP = mean pulmonary arterial pressure, dPAP = diastolic pulmonary arterial pressure, nc = no change, sPAP = systolic pulmonary arterial pressure, sRVP = systolic right ventricular pressure, dRVP = diastolic right ventricular pressure, PAWP = pulmonary arterial wedge pressure, PVR = pulmonary vascular resistance, TPR = total peripheral resistance, RAP = right atrial pressure, CO = cardiac output.

	normal ranges at rest	**PH groups**				
		1	**2**	**3**	**4**	**5**
mPAP (mmHg)	14 ± 3[1]	≥ 25	≥ 25	≥ 25	≥ 25	≥ 25
sPAP (mmHg)	21 ± 4[1]	↑	↑	↑	↑	↑
dPAP (mmHg)	9 ± 3[1]	↑	↑	↑	↑	↑
sRVP (mmHg)	25 ± 10[2]	-	-	-	-	-
dRVP (mmHg)	4 ± 4[2]	↑	↑	↑	↑	↑
PAWP (mmHg)	8 ± 3[1]	≤15	> 15	≤15	≤15	≤15
PVR (Woods)[3]	0.9 ± 0.4[1]	↑	↑/nc	↑	↑	↑
RAP (mmHg)	3 ± 4[2]	↑[4]	↑[4]	↑[4]	↑[4]	↑[4]
CO (L/min)	7 ± 2[1]	↓	nc	↓	↓	↓

[1] data taken from (3); patients were in supine position, values are given as mean ± 1 SD.

[2] data taken from (14), values are given as mean ± 1 SD.

[3] 1 hybrid (Wood) unit = 80×dyne×cm×s^{-5} (15)

[4] in severe cases especially if significant tricuspid regurgitation is present.(13)

Since RHC is an invasive procedure, it carries certain complication risks. Of those complications the vast majority “are mild to moderate in intensity and resolved either spontaneously or after appropriate intervention.” Yet, Hoeper et al. described a 1.1% rate of serious adverse events and a procedure-related mortality of 0.055%.(16)

1.3 Cardiac Magnetic Resonance Phase Contrast Imaging in Pulmonary Hypertension

As recommended in the 2015 ESC/ERS guidelines, echocardiography is the established non-invasive screening tool for patients with suspected PH.(4)

However, echocardiography has major limitations, as the technique is strongly operator dependent and the investigation can be limited by the patients’ body habitus and the absence of appropriate acoustic windows. Cardiac magnetic resonance imaging (CMRI) overcomes these limitations and has emerged as the reference standard technique for the assessment of right ventricular (RV) structure and function.(17–19)

Even though not included in the recommended diagnostic algorithm to pulmonary hypertension in the current guidelines, cardiac MRI enables evaluation of right heart hemodynamic based on the assessment of blood flow velocities.(4)

In recent studies it was shown that the average blood velocity in the MPA derived from magnetic resonance phase contrast imaging (MR-PCI) is strongly correlated with pulmonary arterial pressures and pulmonary vascular resistance, and that pulse wave velocity in the MPA can be measured with good reproducibility. Employing time resolved 3-dimensional MR-PCI of the MPA Reiter et al. found a vortical blood flow in the MPA in patients with PH, which is not observed in patients with normal mPAP. In this study it was shown that the period of existence of MPA vortical blood flow in the cardiac interval strongly correlates with elevated mPAP and enables estimation of mPAP with physical accuracy.(20–22)

Using dedicated software for the evaluation of forward and retrograde blood flow in 2-dimensional (2D) through-plane MR-PCI data of the MPA, Helderman et al. discovered that the early onset of retrograde blood flow in the MPA is significantly

shortened in PAH patients, and provides a reliable non-invasive diagnostic tool to diagnose PAH.(23)

It remains to date unclear, if the early onset of retrograde MPA blood flow is characteristic for PAH only, or if this index can be used to identify PH by 2D MR-PCI in all clinical PH groups.

1.4 Study Hypothesis

The aim of the study was to retrospectively evaluate if the onset of retrograde pulmonary blood flow derived from routine 2D through-plane MR-PCI of the MPA can be evaluated using standard clinical software (Argus Flow, Siemens, Germany), and if the early onset of retrograde flow in the MPA is a diagnostic criterion for PAH only or for PH in general.

2 Materials and Methods

2.1 Study Population

The retrospective study was approved by the local ethical review board (EK Nr. 25-513 ex 12/13). 108 patients (33 male; age, 60 ± 12 years; age range 23 - 82 years) who underwent RHC due to the clinical suspicion of PH and who underwent cardiac magnetic resonance imaging around the time of the RHC were enrolled. No clinically relevant changes in drug treatment or disease state occurred between the examinations. The time delay between the investigations was 11 ± 19 days.

RHC diagnosed PH in 54 patients. 38 patients with mPAP < 21 mmHg (mPAP = 14 ± 4 mmHg; range, 8 – 19 mmHg) and 16 patients who demonstrated borderline mPAP (mPAP = 22 ± 1 mmHg; range, 21 – 24 mmHg) were labelled as non-PH. The demographic characterisation and RHC-derived hemodynamic parameters of the study population are summarised in Table 3 and Table 4.

Table 3: Demographic characterisation of the study population and RHC data. Δ = difference, btw. = between, BSA = body surface area, sPAP = systolic pulmonary artery pressure, dPAP = diastolic pulmonary artery pressure, mPAP = mean pulmonary artery pressure, PAWP = Pulmonary wedge pressure, RAP = right atrial pressure, PVR = pulmonary vascular resistance, CI = cardiac index, sBP = systolic blood pressure, dBP = diastolic blood pressure.

parameter[1]	all	non-PH	PH	PAH	non-PAH PH
Δ of time btw. RHC and MRI (days)	11 ± 19	9 ± 16	12 ± 21	11 ± 26	12 ± 16
age (years)	60 ± 12	57 ± 13	62 ± 12	60 ± 10	64 ± 13
height (cm)	167 ± 8	167 ± 8	167 ± 9	166 ± 7	168 ± 10
weight (kg)	75 ± 16	75 ± 17	75 ± 15	71 ± 11	79 ± 17
BSA[2] (m^2)	1.9 ± 0.22	1.9 ± 0.23	1.9 ± 0.21	1.8 ± 0.16	1.9 ± 0.24
heart rate (1/min)	74 ± 12	71 ± 10	77 ± 13	75 ± 13	79 ± 14
sPAP (mmHg)	46 ± 25	27 ± 7	64 ± 22	67 ± 20	62 ± 23
dPAP (mmHg)	18 ± 10	11 ± 3.2	26 ± 8	26 ± 9	25 ± 8
mPAP (mmHg)	28 ± 15	17 ± 4.2	40 ± 12	41 ± 12	39 ± 12
PAWP (mmHg)	9 ± 5	8 ± 3.0	11 ± 6	9 ± 4.5	12 ± 7
RAP (mmHg)	6 ± 4.3	4.9 ± 3.2	7 ± 4.9	6 ± 4.8	8 ± 4.9
PVR (Woods)[3]	4.1 ± 3.9	1.7 ± 0.78	7 ± 4.2	7 ± 5.0	6 ± 3.3
CI (l/min/m²)	2.9 ± 0.76	3.2 ± 0.75	2.6 ± 0.64	2.8 ± 0.79	2.4 ± 0.40
sBP (mmHg)	127 ± 19	125 ± 17	130 ± 21	125 ± 17	134 ± 23
dBP (mmHg)	64 ± 11	64 ± 10	65 ± 12	62 ± 10	67 ± 14

[1] Values are given as means ± 1 SD.

[2] BSA calculated from Mosteller formula.(24)

[3] 1 hybrid (Wood) unit = 80 dyne×cm×s^{-5} (15)

2.2 Right Heart Catheterisation

2.2.1 Right Heart Catheterisation of the Study Population

Routine RHC was performed in all patients in the Department of Pulmonology, Medical University of Graz. Parameters that were obtained included mPAP, systolic (sPAP) and diastolic (dPAP) pulmonary arterial pressure, pulmonary arterial wedge pressure (PAWP), right atrial pressure (RAP), and pulmonary vascular resistance (PVR) as well as, the cardiac output (CO) measured by thermodilution. RHC based

hemodynamic characterisation and clinical classification of patients taken from pulmonological patient reports are summarised in Table 4 and Figure 1.

Table 4: RHC data and clinical classification of the study population. No. = number of patients, sPAP = systolic pulmonary artery pressure, dPAP = diastolic pulmonary artery pressure, mPAP = mean pulmonary artery pressure, PAWP = Pulmonary wedge pressure, RAP = right atrial pressure, PVR = pulmonary vascular resistance, CI = cardiac index, sBP = systolic blood pressure, dBP = diastolic blood pressure

parameter[1]	**Group 1**	**Group 2**	**Group 3**	**Group 4**	**Group 5**
No. (female)	25 (17)	10 (6)	9 (4)	5 (3)	5 (2)
Heart rate (1/min)	75 ± 13	75 ± 12	76 ± 16	89 ± 12	83 ± 8
sPAP (mmHg)	67 ± 20	55 ± 23	56 ± 19	84 ± 24	63 ± 20
dPAP (mmHg)	26 ± 9	23 ± 7	25 ± 7	31 ± 7	27 ± 8
mPAP (mmHg)	41 ± 12	36 ± 11	35 ± 10	50 ± 12	40 ± 12
PAWP (mmHg)	9 ± 4.5	18 ± 4.9	9 ± 5.0	9 ± 5	8 ± 4.6
RAP (mmHg)	6 ± 4.8	10 ± 4.7	6 ± 2.4	11 ± 7	6 ± 4.2
PVR (Woods)	7 ± 5.0	3.8 ± 2.0	6 ± 2.3	10 ± 1.9	8 ± 4.9
CI (l/min/m²)	2.8 ± 0.79	2.5 ± 0.50	2.3 ± 0.37	2.3 ± 0.27	2.5 ± 0.41
sBP (mmHg)	125 ± 17	147 ± 26	128 ± 20	128 ± 22	127 ± 15
dBP (mmHg)	62 ± 10	75 ± 13	59 ± 14	70 ± 12	62 ± 10

[1] Values are given as means ± 1 SD.

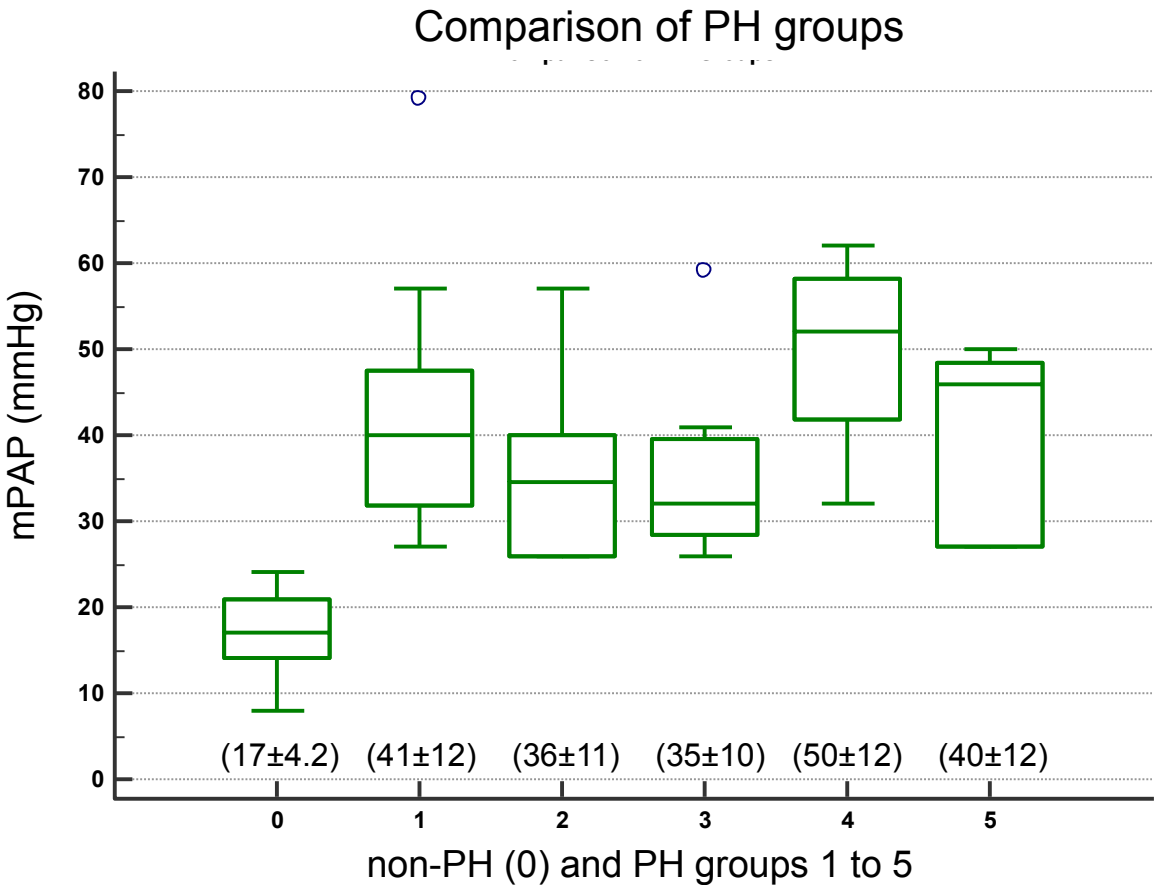

Figure 1: Comparison of the mPAP between patients of the clinical groups of the study population. 0 = non-PH (mPAP < 25 mmHg), 1 = PAH, 2 = PH due to left heart diseases, 3 = PH due to lung diseases, 4 = CTEPH, 5 = PH due to multifactorial of unclear aetiology. The values in brackets are mean values of mPAP (mmHg) of each group ± 1 SD; PH = pulmonary hypertension, PAH = pulmonary arterial hypertension, mPAP = mean pulmonary arterial pressure, CTEPH = chronic thromboembolic pulmonary hypertension.

2.3 Cardiac Magnetic Resonance Phase Contrast Imaging of the Pulmonary Artery

2.3.1 2D MR-PCI Sequence

Electrocardiographically (ECG) gated cardiac MRI investigation of all patients was performed by a 1.5-T MR scanner (Magnetom Sonata; Siemens, Erlangen, Germany) with a six-channel cardiac phased-array coil. Patients were investigated in the supine position. MR-PCI data of the MPA were acquired in breath hold using

a retrospectively ECG-gated, 2D spoiled gradient-echo-based through-plane velocity encoded cine phase-contrast sequence (velocity encoding, 90-180 cm/s; repetition time, 77 ms interpolated to 30 cardiac phases; echo time, 2.8 ms; flip angle, 25°; band width, 385 Hz; typical voxel size, 2.4×1.7×6 mm^3, acquisition time, 19 heart beats). Velocity encoding was adapted if necessary to prevent aliasing artefacts in the MPA. In case a patient was not able to hold his/her breath, threefold averaging was used to suppress breathing artefacts.

2.3.2 MR-PCI of the Main Pulmonary Artery

The image orientation of 2D through-plane velocity encoded MR-PCI of the MPA was adjusted perpendicular to the course of the MPA, approximately 2 cm above the pulmonary valve and below the bifurcation of the MPA. To ensure correct image plane adjustment and position, MR-PCI slices could be displayed on respective cine series of the right ventricular outflow tract and right ventricular 2-chamber view (see Figure 2).

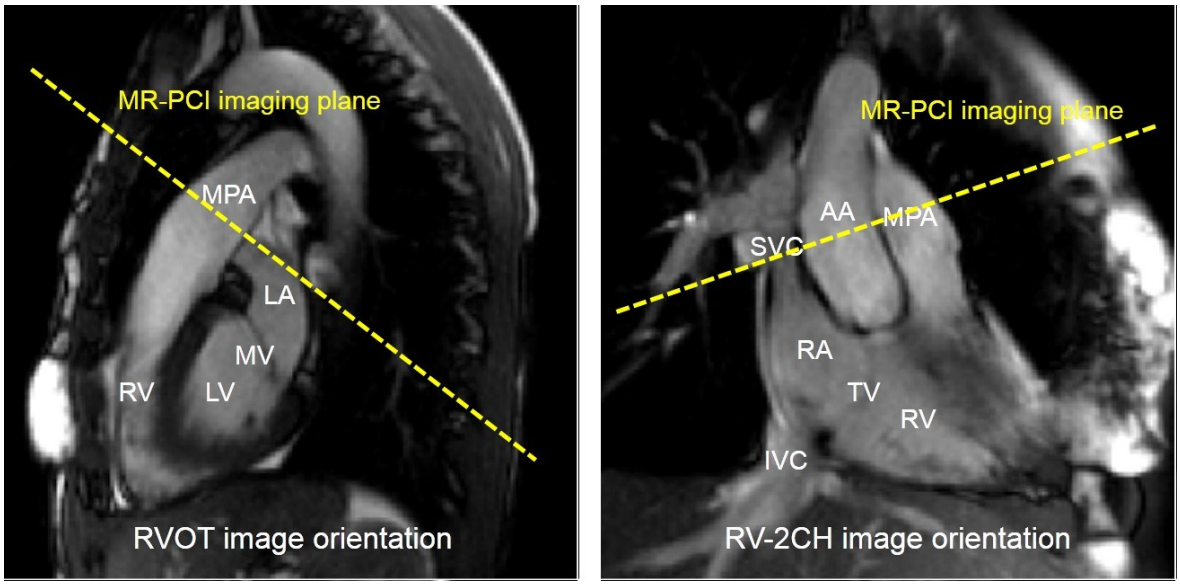

Figure 2: Orientation of 2D through-plane velocity encoded MR-PCI of the main pulmonary artery (MPA). Image orientation is displayed on a right ventricular outflow tract (RVOT) image (left) and right ventricular 2-chamber view (RV-2CH) image (right) in the end-systolic cardiac phase. The line indicates the position of the respective MPA MR-PCI (see Figure 3). AA = ascending aorta, LA = left atrium, LV = left ventricle, PV = pulmonary valve, RV = right ventricle, TV = tricuspid valve, IVC = inferior vena cava, SVC = superior vena cava.

Since the MPA is a relatively short vessel, the position of the MR-PCI imaging plane was crucial for data evaluation. In correctly orientated and positioned images, the MPA is displayed with circular cross-section (Figure 3).

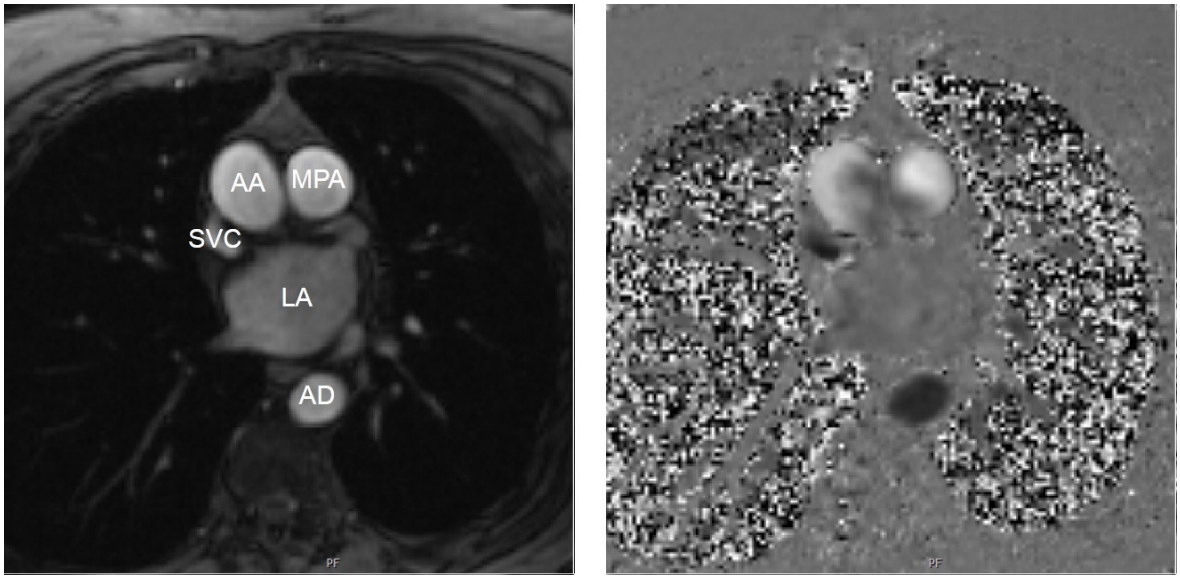

Figure 3: Typical systolic 2D through-plane velocity encoded MR-PCI of the MPA. Re-phased (anatomical) image (left) and phase image (right). AA = ascending aorta, AD = descending aorta, MPA = main pulmonary artery, LA = left atrium, SCV = superior vena cava.

The MR-PCI plane should not be too close to the pulmonary valve to avoid motion of the valve leaflets into the MPA vessel cross-section and to minimise the interference of the valvular vortical blood flow with MPA flow patterns. On the other hand, the image plane should not cross the bifurcation of the MPA. As the vessel moves throughout the cardiac cycle, image position was reviewed in end-systole.

If an investigation revealed multiple, repeated MPA MR-PCI acquisitions, the image that best fulfilled the aspects mentioned above was chosen (Figure 4).

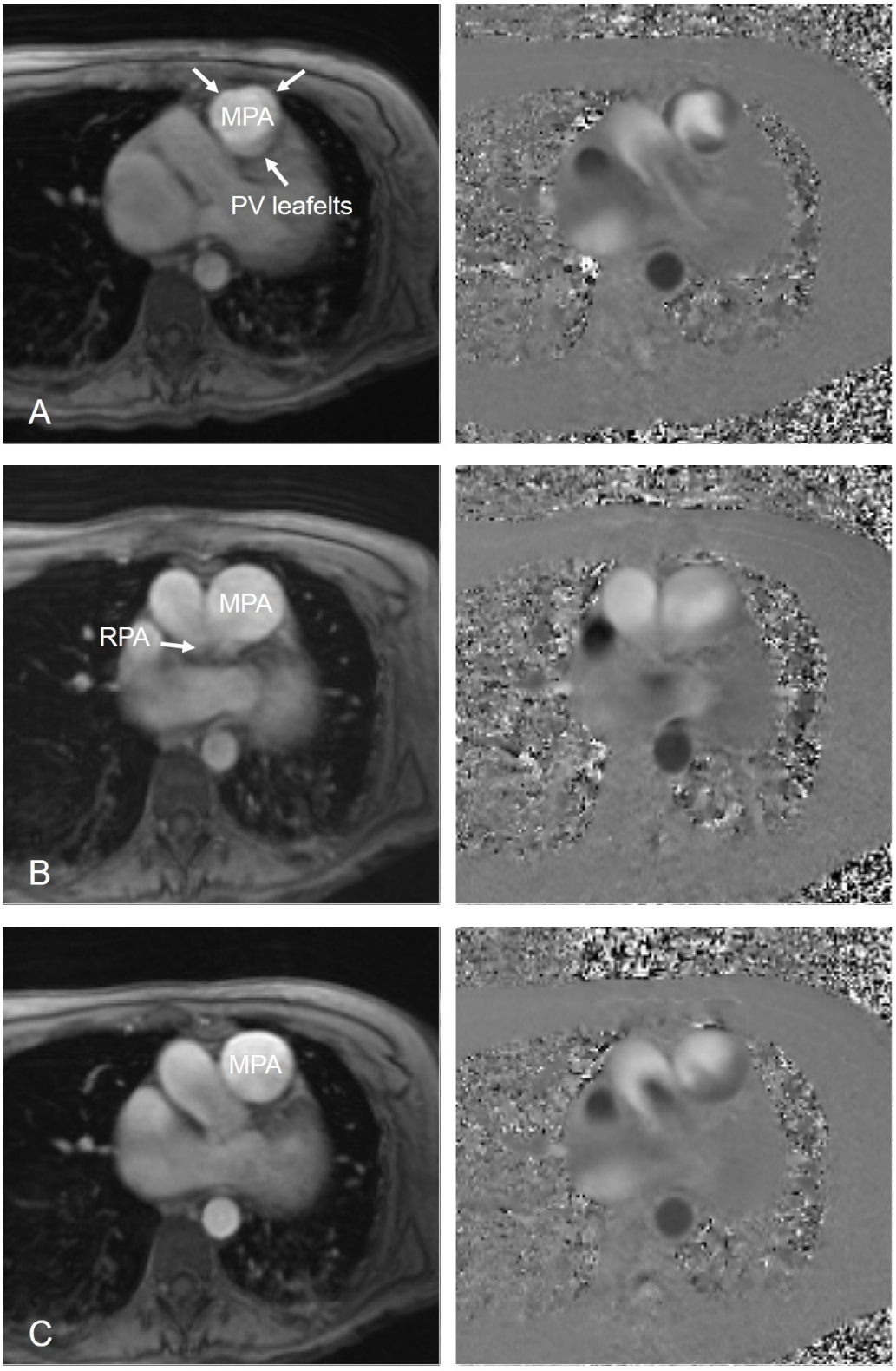

Figure 4: Selection of MPA MR-PCI data for evaluation. Re-phased images (left) and phase images (right) in end-systole. Image plane positioned too close to the pulmonary valve (A), plane positioned too high crossing the bifurcation of the MPA (B) and respective repeated, corrected image (C). MPA = main pulmonary artery, RPA = right pulmonary artery branch, PV = pulmonary valve.

2.4 Evaluation of Pulmonary Artery Phase Contrast Data

2.4.1 MRI-PCI Data Evaluation

MR-PCI of the MPA were evaluated by routine evaluation software ARGUS FLOW VA60C (Siemens Healthcare GmbH, Erlangen, Germany). Anatomical and phase images were juxtaposed. The MPA vessel cross-section was segmented in the anatomical images throughout the cardiac cycle (Figure 5). The segmentation was automatically transferred to the respective phase images. After segmentation of all images, time courses of the vessel cross-section, mean velocity, peak velocity, MPA blood flow, as well as forward, backward, and net forwards blood volumes were calculated by the software.

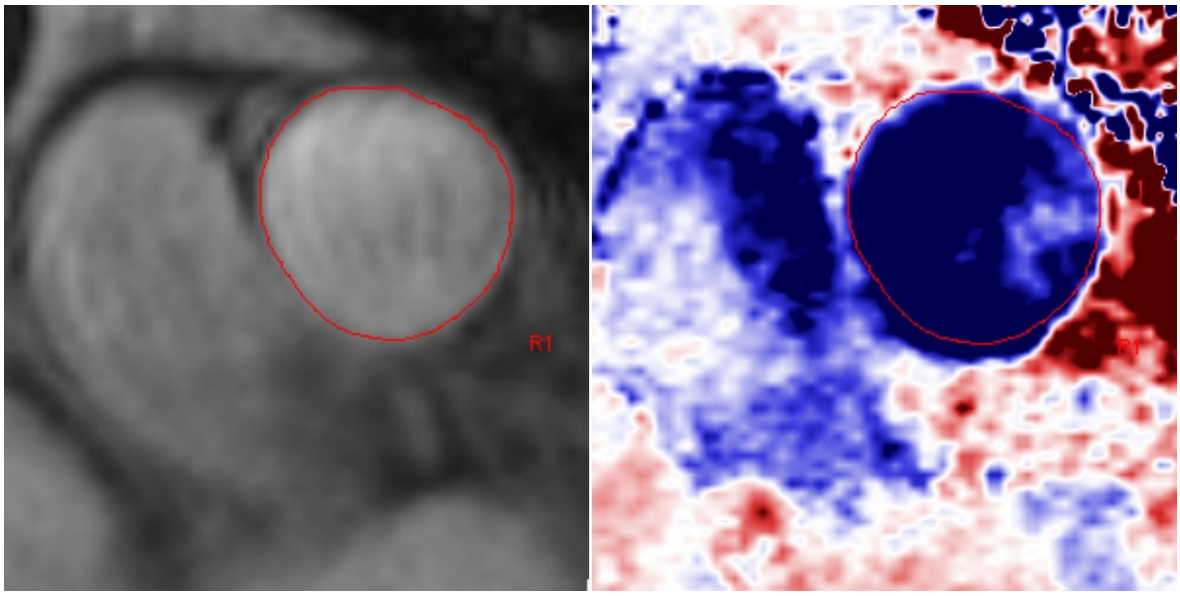

Figure 5: MPA MR-PCI data evaluation. The images display a re-phased (right) and phase (left) image of a systolic cardiac phase. Region of interest (ROI 1, red line) was manually segmented on the anatomical image (left) and contours were automatically transferred to the phase image. Velocity in the phase image is displayed colour encoded (red/blue) visualising through-plane forward (blue) and through-plane retrograde (red) blood flow. R1 = segmented MPA cross-section area.

2.4.2 Evaluation of Retrograde Blood Flow

For separation of MPA forward and retrograde flow, the centre of contrast was set to zero in the phase image and the velocity display was switched to red/blue velocity colour representation (Figure 5 and Figure 6). Areas of retrograde velocity within the MPA cross-section were manually outlined (ROI 2), starting at the systolic phase with maximum retrograde flow. MPA contours (ROI 1) were used to identify the border of ROI 2 towards the ascending aorta, the pericardial fat and the lung, which could not be correctly identified in the velocity encoded images. Retrograde flow was traced image by image in all slices, until onset at earlier and extinction at later cardiac phases. Only the retrograde flow areas, which led to and came from the major retrograde flow, were outlined to avoid valvular blood flow patterns in ROI 2. After segmentation, time courses of the retrograde mean velocity, retrograde peak velocity, and retrograde flow were calculated by the ARGUS FLOW software.

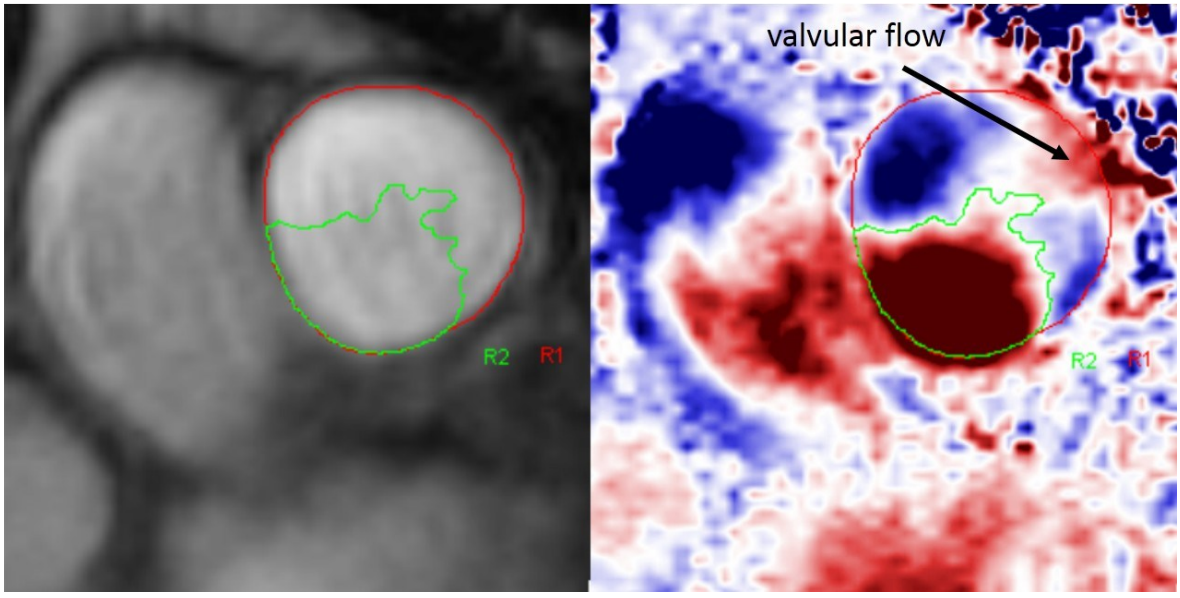

Figure 6: Evaluation of retrograde blood flow in the main pulmonary artery. The images display a systolic cardiac phase. Red/blue through-plane velocity colour encoding enabled segmentation of retrograde flow in the MPA (green line). R1 = MPA cross-section area, R2 = area with retrograde flow in the MPA.

2.4.3 Retrograde MPA Blood Flow Onset Time

Results from ARGUS FLOW evaluation including time courses of MPA (ROI 1) and retrograde (ROI 2) flow were exported as text and evaluated with Excel software (Microsoft Corporation, Redmond, USA). MPA and retrograde blood flow time courses were imported into a dedicated post-processing worksheet (Reiter G., DataEvaluationSheet_RetroFlow). The program displayed normalised flow vs. time courses of both, MPA and retrograde flow, enabling to identify and exclude data point arising from pulmonary valve (Figure 4A) or noise.

Since it was not clear how to determine onset times of retrograde flow (ROT), four different algorithms were tested: a threshold based algorithm, a half-maximum based algorithm, and two different upslope-fit algorithms.

2.4.3.1 The Threshold Algorithm

ROT was determined from the time when a threshold of flow was exceeded (Figure 7). Thresholds tested were 5% (0.05) and 10% (0.1) of MPA and retrograde flow, respectively and corrected manually if needed. The ROT_{TH} was automatically calculated by the program as the difference of MPA and retrograde stating times. Moreover, the relative onset time $rROT_{TH}$ was derived referring ROT_{TH} to the duration of the cardiac interval.

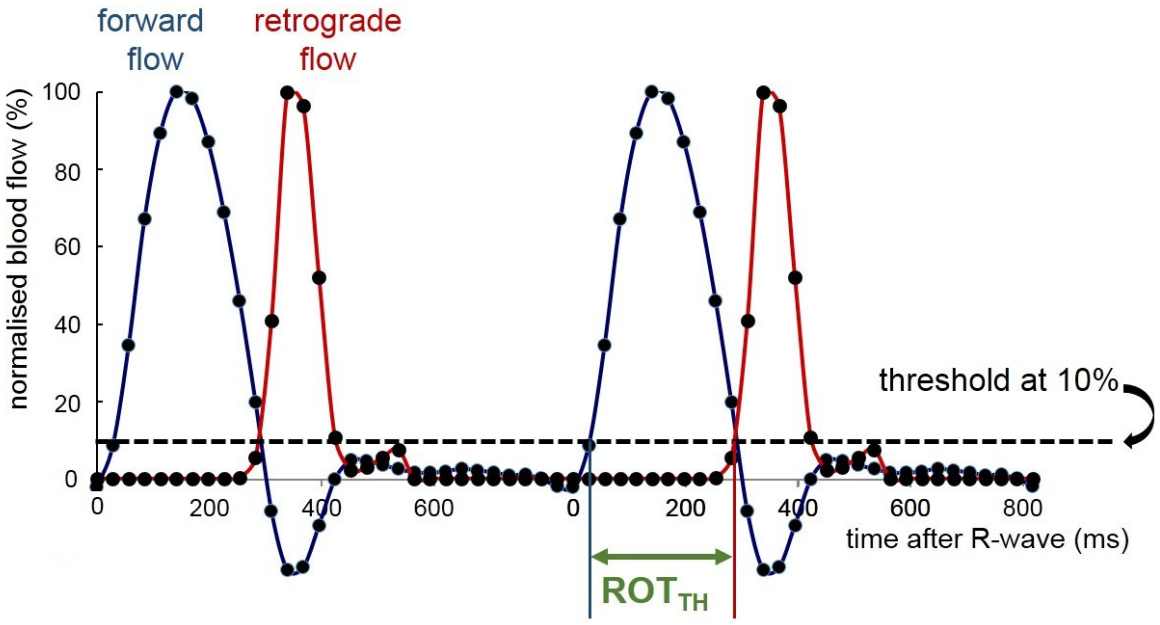

Figure 7: Threshold algorithm for calculation of onset time of retrograde flow in the MPA. Normalised MPA flow (blue curved line, ROI 1) and retrograde flow (red curved line, ROI 2). Here a threshold of 10% determines the retrograde flow onset time (ROT) as the difference between MPA forward (ROI 1) and retrograde (ROI 2) blood flow starting time.

2.4.3.2 The Half-Maximum Algorithm

The ROT can also be calculated as the time difference between half-maxima of MPA and retrograde flow curves (ROT_{HM}). Half-maximum times of the flow curves were calculated automatically (Figure 8). The search interval for finding the half-maximum was manually adapted. Moreover, the relative onset time $rROT_{HM}$ was derived referring ROT_{HM} to the duration of the cardiac interval.

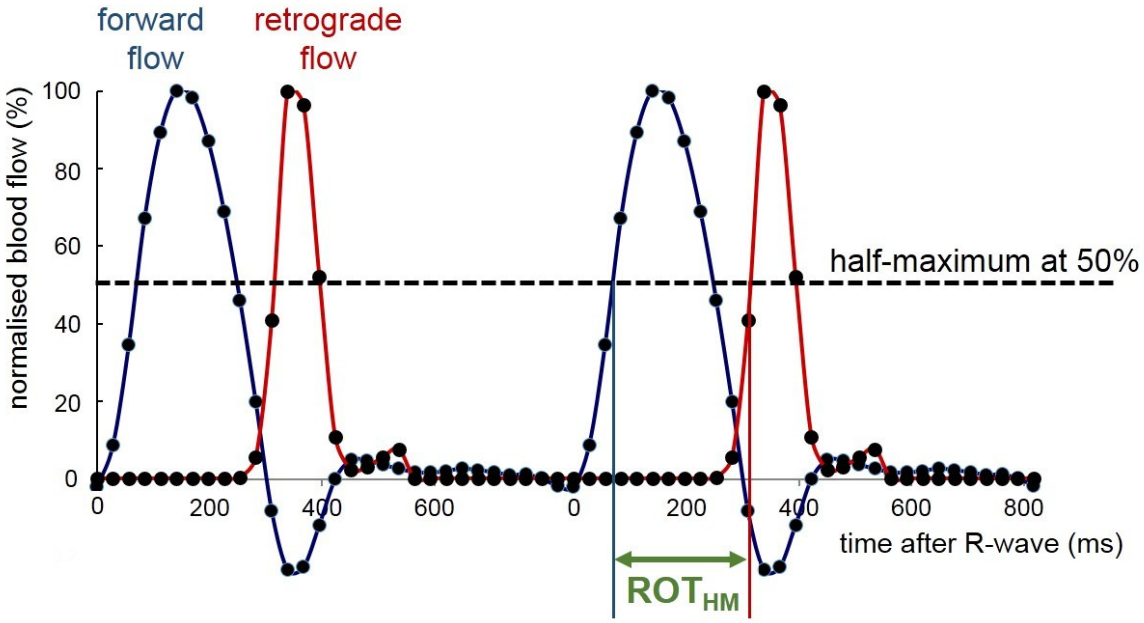

Figure 8: Half-maximum algorithm for calculation of onset time of retrograde flow in the MPA. Normalised MPA flow (blue curved line, ROI 1) and retrograde flow (red curved line, ROI 2). Here, the half-maximum determines the retrograde flow onset time (ROT) as the difference between 50% MPA forward (ROI 1) and 50% retrograde (ROI 2) blood flow.

2.4.3.3 Linear Extrapolation below Half-Maximum Algorithm

Onset times of MPA forward and retrograde blood flow were evaluated from linear extrapolation of flow curves below the half-maxima (ROT_{HMUS}). The number of data points was manually chosen. Linear fit and extrapolation towards 0% flow (y=0) defined the starting times of respective flow curves (Figure 9). Moreover, the relative onset time $rROT_{HMUS}$ was derived referring ROT_{HMUS} to the duration of the cardiac interval.

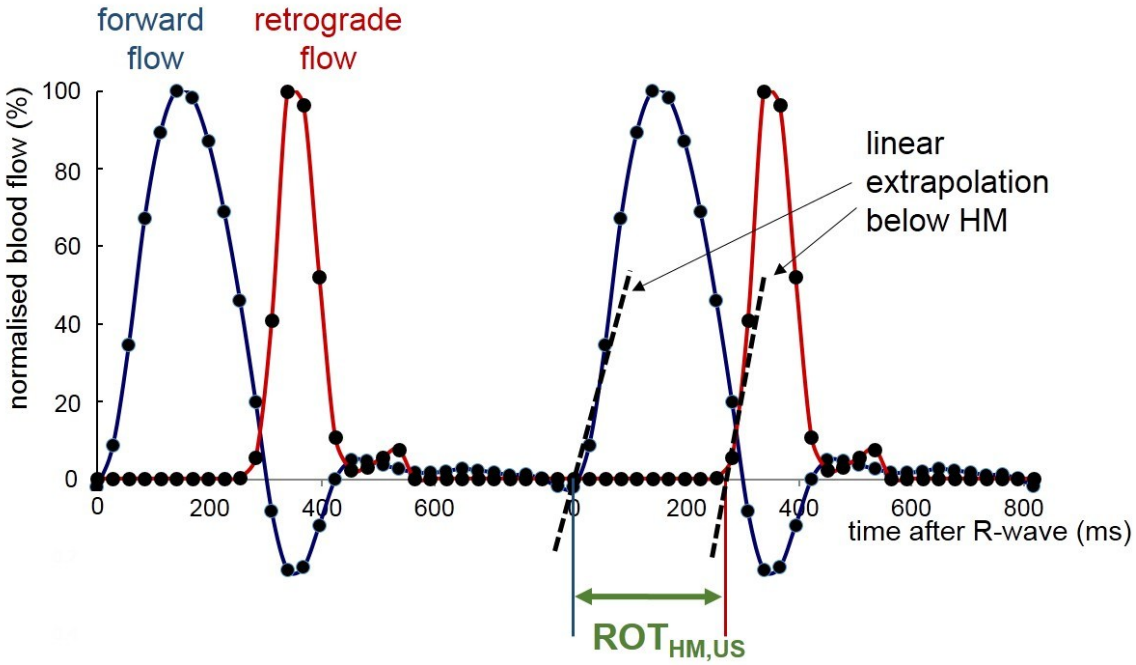

Figure 9: Linear extrapolation below half-maximum for calculation of onset time of retrograde flow in the MPA. ROT is calculated as the time difference between onset of MPA flow (blue curved line, ROI 1) and retrograde flow (red curved line, ROI 2) is derived from curve fit and extrapolation to 0% flow.

2.4.3.4 Full Upslope Linear Extrapolation Algorithm

Onset times of MPA forward and retrograde blood flow were evaluated from linear extrapolation of the entire upslope of the respective flow curves (ROT_{US}). The number of data points was manually chosen. Linear fit and extrapolation towards 0% flow (y=0) defined the starting times of MPA and retrograde flow curves (Figure 10). Moreover, the relative onset time $rROT_{US}$ was derived referring ROT_{US} to the duration of the cardiac interval.

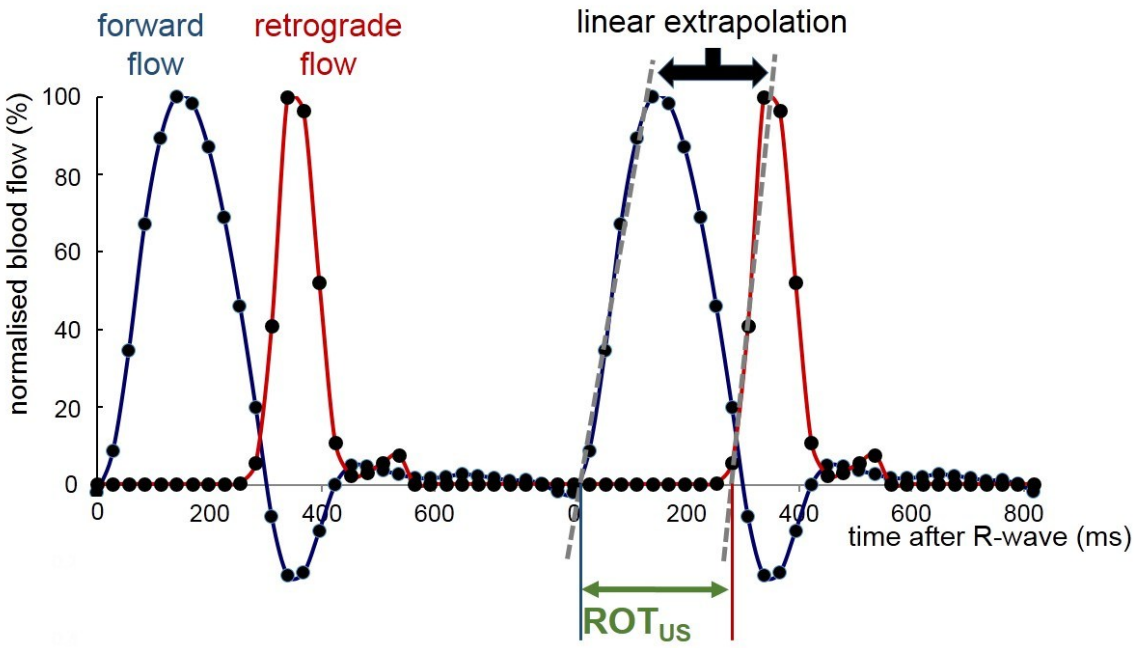

Figure 10: Full upslope linear extrapolation for calculation of onset time of retrograde flow in the MPA. ROT is calculated as the time difference between onset of MPA flow (blue curved line, ROI 1) and retrograde flow (red curved line, ROI 2) blood flow is derived from upslope curve fit and extrapolation to 0% flow.

2.5 Statistical Analysis

Mean values are given with ± 1 SDs. Statistical analysis was performed with statistical software (MedCalc Vers. 15.8, MedCalc Software bvba). For statistical tests a significance level of 0.05 was used.

Mean values of the ROTof the groups non-PHand PH, as well as PAH and non-PAH PH patients were compared using a two-sample t-test. The relationship between ROT and mPAP was analysed by correlation and linear regression analysis.

Receiver operating characteristic (ROC) curve analysis was performed to investigate the diagnostic performance of ROT to diagnose PH within all patients, within PAH and non-PH patients and within non-PAH PH and non-PH patients. Cut-offs were determined by maximizing diagnostic accuracy; corresponding sensitivities and specificities for these cut-offs were given.

3 Results

3.1 Standard MPA MR-PCI Parameter

Standard parameters of MR-PCI data of the MPA including vessel cross-section area, peak and average blood velocities and blood volumes were evaluated in all patients. Average, minimal, and maximal MPA cross-section area were significantly larger in PH compared to non-PH patients ($p < 0.0001$) but did not differ between PAH and non-PAH PH patients ($p = 0.60$, 0.54 and 0.68 for average, minimal and maximal MPA cross-section area). Moreover, mean MPA blood velocity was significantly lower in PH compared to the non-PH patients ($p = 0.0001$). Results of the MPA MR-PCI measurements are summarised in Table 5.

Table 5: Standard parameters from MPA MR-PCI data. PH = pulmonary hypertension, PAH = pulmonary arterial hypertension, min = minimum, max = maximum.

parameter[1]	**all**	**non-PH**	**PH**	**PAH**	**non-PAH PH**
area (cm^2)					
-average	7 ± 3.1	6 ± 1.7	9 ± 3.3	9 ± 3.3	9 ± 3.3
-min	6 ± 3.0	4.8 ± 1.6	8 ± 3.2	8 ± 3.4	8 ± 3.1
-max	8 ± 3.4	7 ± 1.9	10 ± 3.6	10 ± 3.5	10 ± 3.6
mean velocity (cm/s)					
-mean min	-2.1 ± 5.0	-2.4 ± 7	-1.8 ± 2.3	-1.8 ± 2.1	-1.9 ± 2.4
-mean max	41 ± 15	46 ± 15	35 ± 13	35 ± 12	35 ± 13
peak velocity (cm/s)					
-max	64 ± 35	66 ± 31	63 ± 38	58 ± 48	67 ± 26
blood volume (cm^3)					
-net forward	62 ± 28	63 ± 27	61 ± 29	61 ± 36	61 ± 24
-retrograde	2.6 ± 6	2.1 ± 7	3.2 ± 4.7	4.1 ± 6	2.4 ± 3.3

[1] Values are given as means ± 1 SD.

3.2 MPA Retrograde Blood Flow Onset Times

3.2.1 Threshold Retrograde Onset Times

Absolute and relative ROT derived from threshold analysis were calculated and analysed for non-PH vs. PH and PAH vs. non-PAH PH patients. Absolute (Figure 11 & Figure 12) and relative ROT_{TH} values significantly differed between non-PH and PH patients (ROT_{TH} for non-PH and PH were 345 ± 74 ms and 237 ± 85 ms, $p < 0.0001$; $rROT_{TH}$ for non-PH and PH were 0.39 ± 0.09 and 0.28 ± 0.11, $p < 0.0001$). No significant difference in either ROT_{TH} or $rROT_{TH}$ was found between PAH and non-PAH PH groups (ROT_{TH} for PAH and non-PAH PH were 227 ± 85 ms and 246 ± 86 ms, $p = 0.4222$; $rROT_{TH}$ for PAH and non-PAH PH were 0.26 ± 0.10 and 0.30 ± 0.11, $p = 0.1538$).

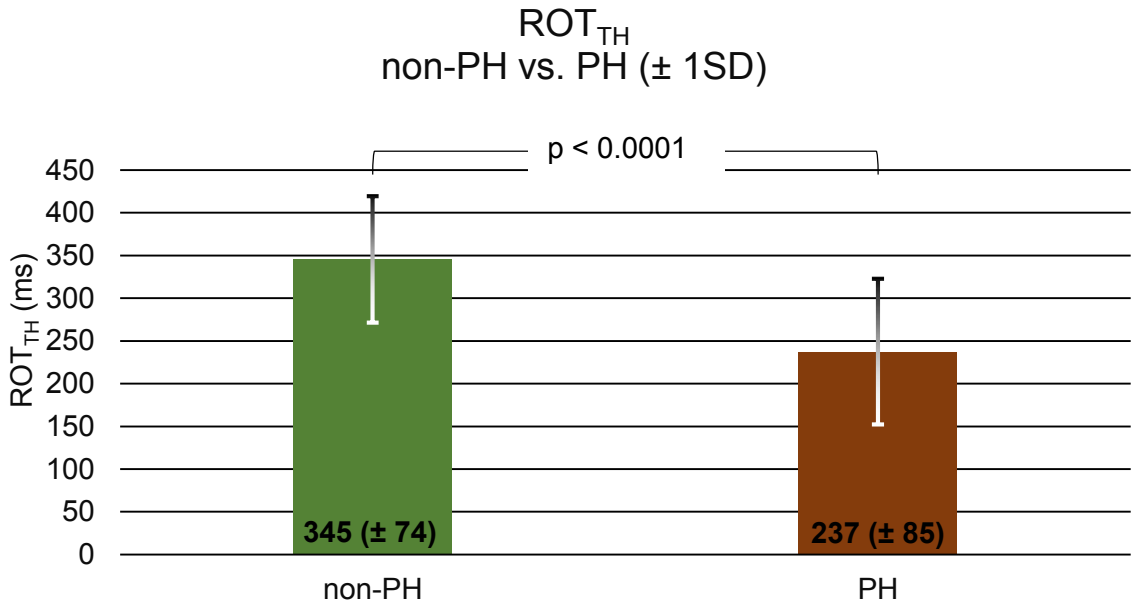

Figure 11: Comparison of ROT_{TH} of non-PH and PH patients. PH = pulmonary hypertension, ROT_{TH} = threshold derived onset time of retrograde flow in the main pulmonary artery. Mean values given with ± 1SD.

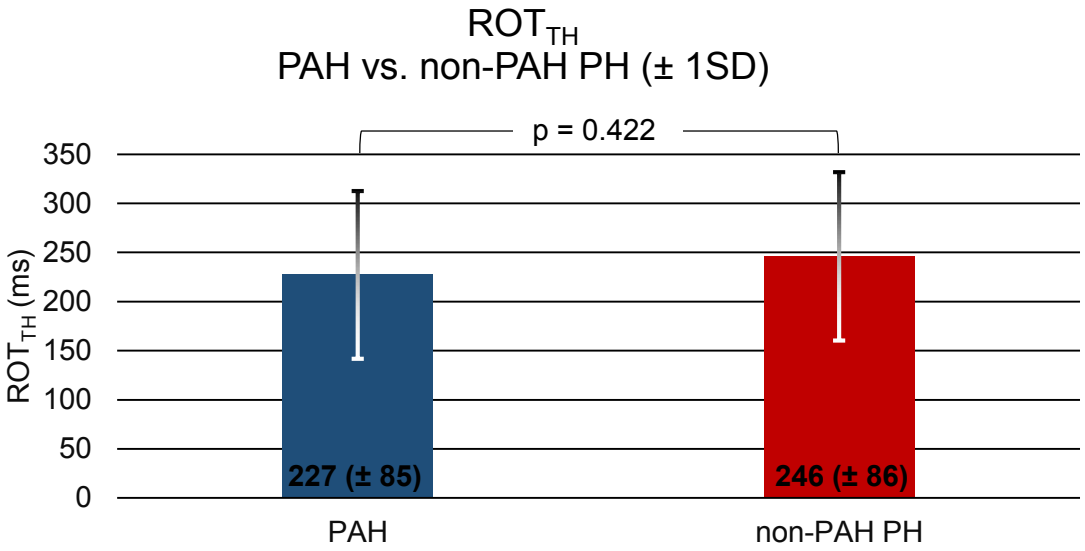

Figure 12: Comparison of ROT$_{TH}$ of PAH and non-PAH PH patients. PH = pulmonary hypertension, PAH = pulmonary arterial hypertension. ROT$_{TH}$ = threshold derived onset time of retrograde flow in the main pulmonary artery. Mean values given with ± 1SD.

3.2.2 Half-Maximum Retrograde Onset Times

Absolute and relative ROT derived from half-maximum analysis were calculated and analysed for non-PH vs. PH and PAH vs. non-PAH PH patients. Absolute (Figure 13 & Figure 14) and relative ROT$_{HM}$ values significantly differed between non-PH and PH patients (ROT$_{HM}$ for non-PH and PH were 269 ± 52 ms and 208 ± 75 ms, $p < 0.0001$; rROT$_{HM}$ for non-PH and PH were 0.30 ± 0.06 and 0.24 ± 0.08, $p = 0.0001$). No significant difference in either ROT$_{HM}$ or rROT$_{HM}$ was found between PAH and non-PAH PH groups (ROT$_{HM}$ for PAH and non-PAH PH were 205 ± 76 ms and 212 ± 75 ms, $p = 0.7442$; rROT$_{HM}$ for PAH and non-PAH PH were 0.23 ± 0.08 and 0.25 ± 0.08, $p = 0.3252$).

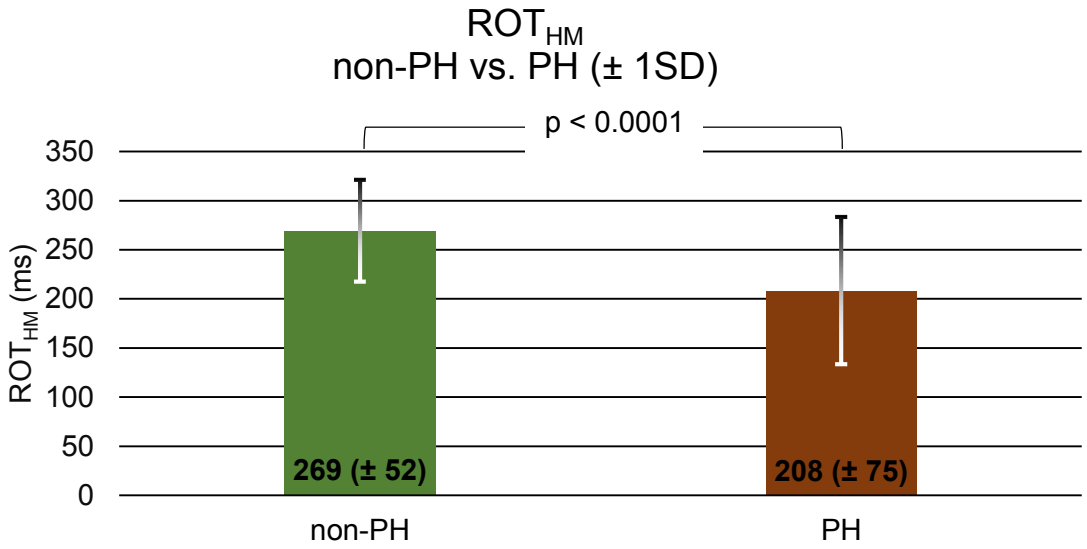

Figure 13: Comparison of ROT_{HM} of non-PH and PH patients. PH = pulmonary hypertension, ROT_{HM} = half-maximum derived onset time of retrograde flow in the main pulmonary artery. Mean values given with ± 1SD.

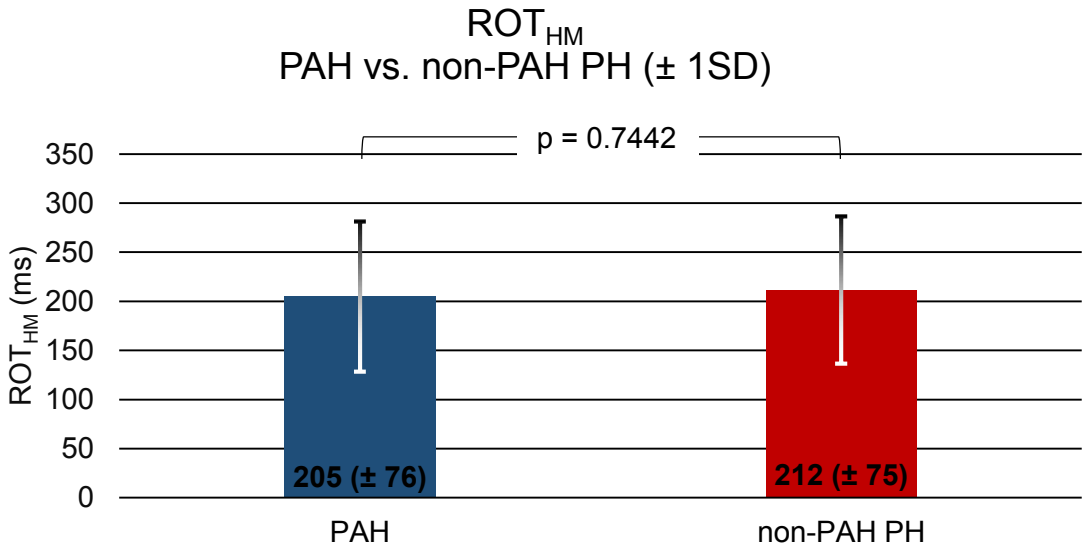

Figure 14: Comparison of ROT_{HM} of PAH and non-PAH PH patients. PH = pulmonary hypertension, PAH = pulmonary arterial hypertension. ROT_{HM} = half-maximum derived onset time of retrograde flow in the main pulmonary artery. Mean values given with ± 1SD.

3.2.3 Linear Extrapolation below Half-Maximum Retrograde Onset Times

Absolute and relative ROT derived from linear extrapolation below half-maximum analysis were calculated and analysed for non-PH vs. PH and PAH vs. non-PAH PH patients. Absolute (Figure 15 & Figure 16) and relative ROT_{HMUS} values significantly differed between non-PH and PH patients (ROT_{HMUS} for non-PH and PH were 259 ± 77 ms and 153 ± 62 ms, $p < 0.0001$; $rROT_{HMUS}$ for non-PH and PH were 0.29 ± 0.10 and 0.18 ± 0.08, $p < 0.0001$). No significant difference in either ROT_{HMUS} or $rROT_{HMUS}$ was found between PAH and non-PAH PH groups (ROT_{HMUS} for PAH and non-PAH PH were 146 ± 68 ms and 158 ± 57 ms, $p = 0.4868$; $rROT_{HMUS}$ for PAH and non-PAH PH were 0.17 ± 0.08 and 0.19 ± 0.07, $p = 0.2623$).

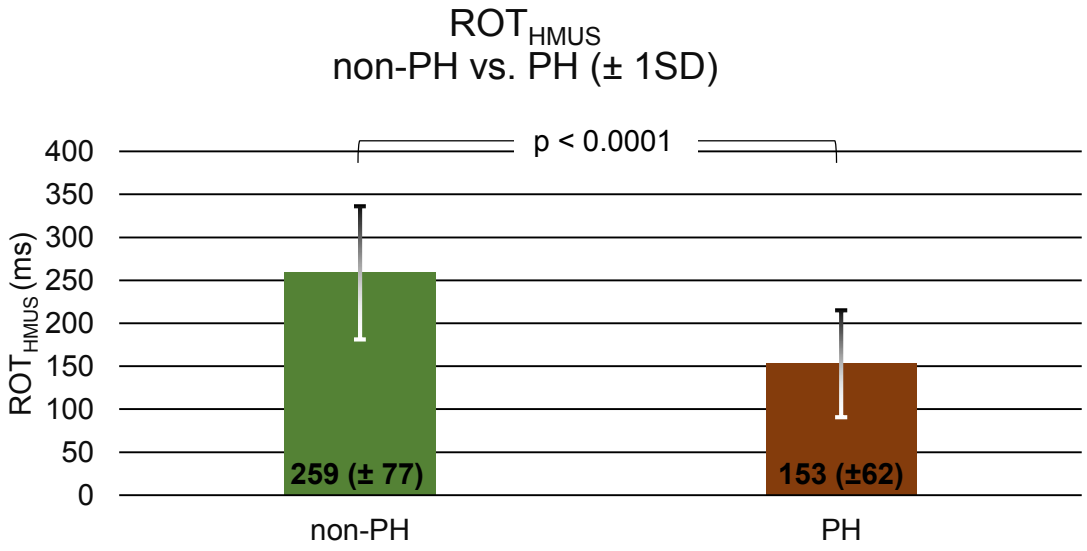

Figure 15: Comparison of ROT_{HMUS} of non-PH and PH patients. PH = pulmonary hypertension, ROT_{HMUS} = linear extrapolation below half-maximum derived onset time of retrograde flow in the main pulmonary artery. Mean values given with ± 1SD.

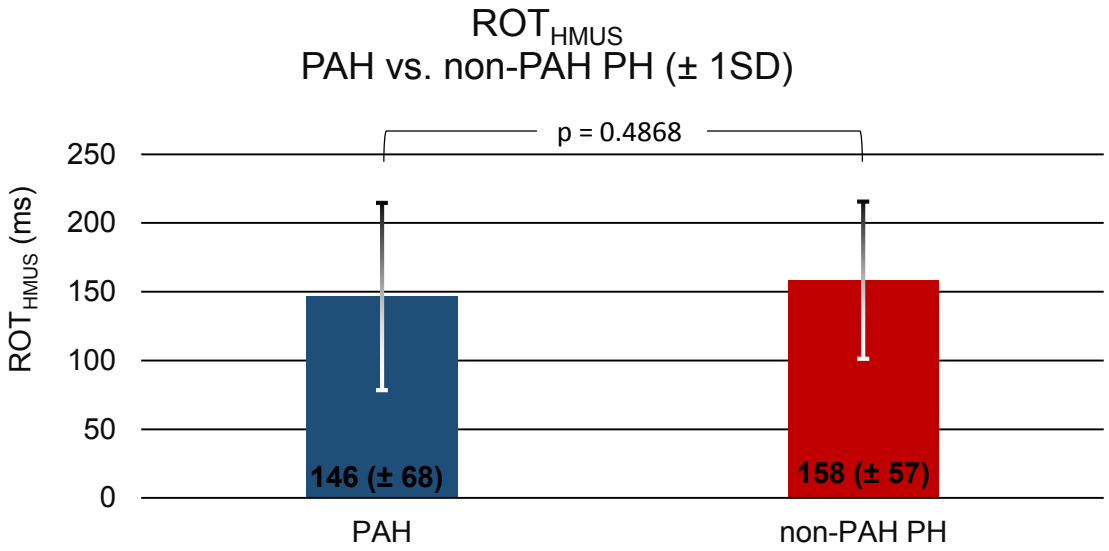

Figure 16: Comparison of ROT_{HMUS} of PAH and non-PAH PH patients. PH = pulmonary hypertension, PAH = pulmonary arterial hypertension. ROT_{HMUS} = linear extrapolation below half-maximum derived onset time of retrograde flow in the main pulmonary artery. Mean values given with ± 1SD.

3.2.4 Full Upslope Linear Extrapolation Retrograde Onset Times

Absolute and relative ROT derived from full upslope linear extrapolation analysis were calculated and analysed for non-PH vs. PH and PAH vs. non-PAH PH patients. Absolute (Figure 17 & Figure 18) and relative ROT_{US} values significantly differed between non-PH and PH patients (ROT_{US} for non-PH and PH were 271 ± 65 ms and 144 ± 53 ms, $p < 0.0001$; $rROT_{US}$ for non-PH and PH were 0.30 ± 0.08 and 0.17 ± 0.07, $p < 0.0001$). No significant difference in either ROT_{US} or $rROT_{US}$ was found between PAH and non-PAH PH groups (ROT_{US} for PAH and non-PAH PH were 138 ± 52 ms and 150 ± 54 ms, $p = 0.4145$; $rROT_{US}$ for PAH and non-PAH PH were 0.16 ± 0.08 and 0.18 ± 0.06, $p = 0.2416$).

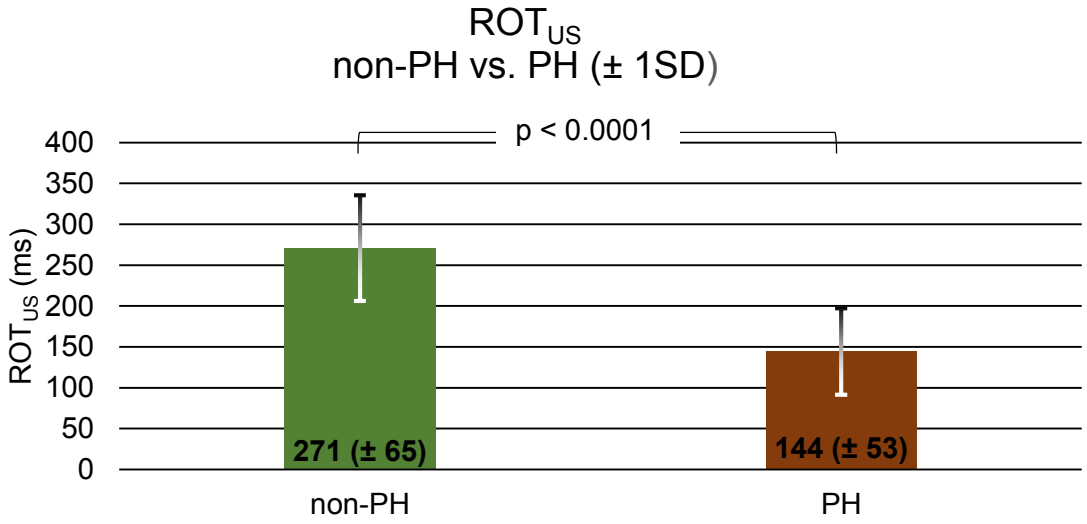

Figure 17: Comparison of ROT_{US} of non-PH and PH patients. PH = pulmonary hypertension, ROT_{US} = full upslope linear extrapolation derived onset time of retrograde flow in the main pulmonary artery. Mean values given with ± 1SD.

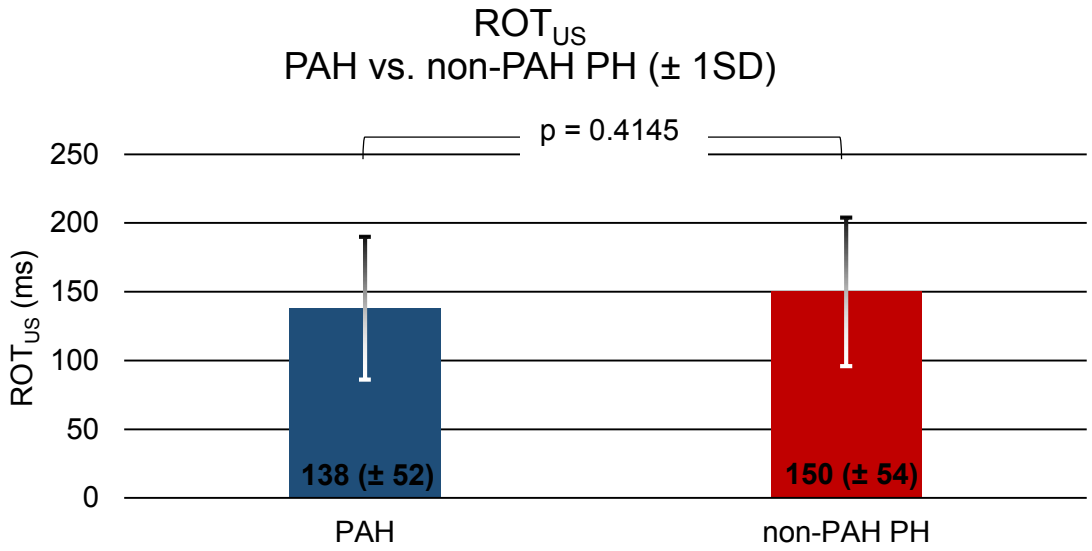

Figure 18: Comparison of ROT_{US} of PAH and non-PAH PH patients. PH = pulmonary hypertension, PAH = pulmonary arterial hypertension. ROT_{US} = full upslope linear extrapolation derived onset time of retrograde flow in the main pulmonary artery. Mean values given with ± 1SD.

3.3 Correlation of ROT with mPAP

Linear regression and correlation analysis revealed moderate negative correlations between ROT and mPAP. The strongest correlations with mPAP in all patients were found with ROT_{US} (r = -0.67) and $rROT_{US}$ (r = -0.60). Restricting the patient population to PH, PAH or non-PAH PH, mPAP was related to ROT only in the PAH group (ROT_{TH}, r = -0.53; ROT_{HM}, r = -0.63; ROT_{HMUS}, r = -0.43; ROT_{US}, r =-0.51). Results of the linear regression and correlation analysis of ROT with mPAP are summarised in Table 6.

Besides the correlations of ROT, MPA cross-section area was positively and mean MPA blood velocity negatively related to mPAP (mean and minimum MPA cross-section area, r = 0.64, maximum MPA cross-section area, r = 0.62, MPA maximum average velocity, r = -0.49). Relations of MR-PCI parameters of the study population with highest correlations with mPAP are shown in Figure 19.

Table 6: Correlation and linear regression analysis of the onset time of retrograde flow with mPAP. ROT = onset time of retrograde blood flow derived from threshold (TH), half-maximum (HM), linear extrapolation below half-maximum (HMUS) and full upslope linear extrapolation (US) algorithms, rROT = onset time of retrograde blood flow relative to the cardiac interval derived from the algorithms as listed above, ic = intercept with x-axis, r = Pearson correlation coefficient.

All patients (n = 108)				**All patients (n = 108)**			
ROT	ic (ms)	slope (ms/mmHg)	r	rROT	ic	slope ($1/10^{-3}$mmHg)	r
ROT_{TH} (ms)	395	-3.66	-0.56	$rROT_{TH}$	0.44	-3.61	-0.47
ROT_{HM} (ms)	299	-2.12	-0.43	$rROT_{HM}$	0.33	-2.00	-0.37
ROT_{HMUS} (ms)	300	-3.33	-0.55	$rROT_{HMUS}$	0.34	-3.49	-0.49
ROT_{US} (ms)	320	-3.96	-0.67	$rROT_{US}$	0.35	-4.10	-0.60
PH (n=54)				**PH (n=54)**			
ROT	ic (ms)	slope (ms/mmHg)	r	rROT	ic	slope ($1/10^{-3}$mmHg)	r
ROT_{TH} (ms)	311	-1.84	-0.26	$rROT_{TH}$	0.36	-1.84	-0.21
ROT_{HM} (ms)	256	-1.19	-0.19	$rROT_{HM}$	0.29	-1.17	-0.16
ROT_{HMUS} (ms)	196	-1.09	-0.21	$rROT_{HMUS}$	0.23	-1.09	-0.16
ROT_{US} (ms)	193	-1.22	-0.27	$rROT_{US}$	0.22	-1.14	-0.20
PAH (n=25)				**PAH (n=25)**			
ROT	ic (ms)	slope (ms/mmHg)	r	rROT	ic	slope ($1/10^{-3}$mmHg)	r
ROT_{TH} (ms)	382	-3.73	-0.53	$rROT_{TH}$	0.38	-2.99	-0.36
ROT_{HM} (ms)	367	-3.92	-0.63	$rROT_{HM}$	0.38	-3.53	-0.50
ROT_{HMUS} (ms)	246	-2.41	-0.43	$rROT_{HMUS}$	0.25	-1.99	-0.28
ROT_{US} (ms)	228	-2.17	-0.51	$rROT_{US}$	0.24	-1.85	-0.30
non-PAH PH (n=29)				**non-PAH PH (n=29)**			
ROT	ic (ms)	slope (ms/mmHg)	r	rROT	ic	slope ($1/10^{-3}$mmHg)	r
ROT_{TH} (ms)	242	0.11	0.01	$rROT_{TH}$	0.31	-0.38	-0.04
ROT_{HM} (ms)	155	1.47	0.23	$rROT_{HM}$	0.20	1.29	0.18
ROT_{HMUS} (ms)	148	0.27	0.05	$rROT_{HMUS}$	0.19	-0.02	0.00
ROT_{US} (ms)	159	-0.22	-0.05	$rROT_{US}$	0.19	0.27	-0.05

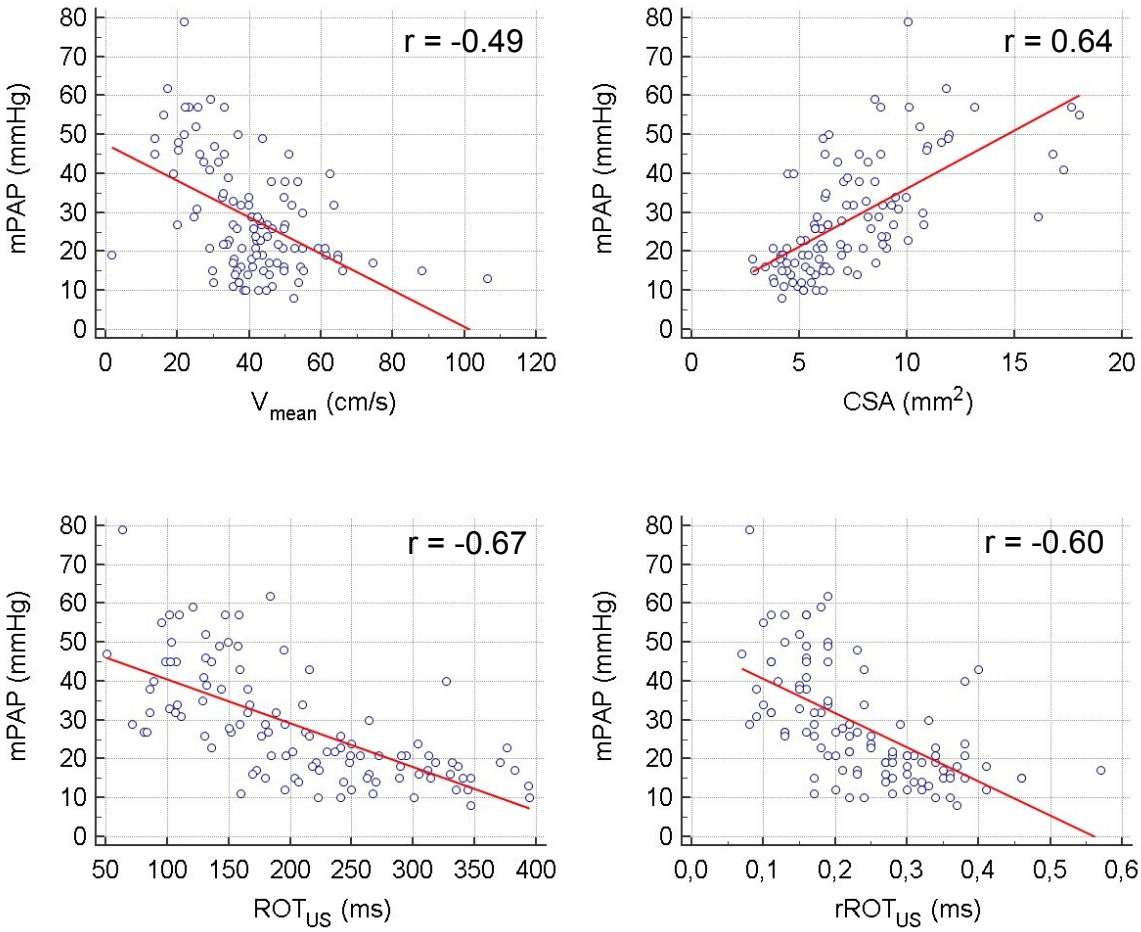

Figure 19: Correlations of MPA and retrograde flow parameters with mPAP. MPA = main pulmonary artery, mPAP = mean pulmonary arterial pressure, r = Pearson correlation coefficient, V_{mean} = maximal mean velocity in the MPA, CSA = average MPA cross-section area, ROT_{US} = onset time of retrograde blood flow derived from full upslope linear extrapolation, $rROT_{US}$ = onset time of retrograde blood flow derived from full upslope linear extrapolation relative to the cardiac interval, red line = linear regression lines.

3.4 Diagnostic Performance of ROT

Receiver operator characteristic (ROC) curves to predict PH from ROT and rROT derived from threshold, half-maximum, linear extrapolation below half-maximum and full upslope linear extrapolation algorithms are summarised in Table 7. Analysis was performed to diagnose PH within all patients, within PAH and non-PH patients and within non-PAH PH and non-PH patients. In all methods and groups ROTs re-

vealed higher AUCs than rROTs. Full upslope linear extrapolation algorithm provided highest AUCs in all patients (AUC = 0.94), non-PH and PAH (AUC = 0.95), as well as non-PH and non-PAH PH (AUC = 0.93). Respective ROC curves are shown in Figure 20.

Table 7: Results of the ROC calculations. PH = pulmonary hypertension, PAH = pulmonary arterial hypertension, AUC = area under ROC curve, ROT = onset time of retrograde blood flow derived from threshold (TH), half-maximum (HM), linear extrapolation below half-maximum (HMUS), and full upslope linear extrapolation (US) algorithms, rROT = onset time of retrograde blood flow relative to the cardiac interval derived from the algorithms same as listed above.

parameter	**PH**		**PAH**		**non-PAH PH**	
ROT	AUC	standard error	AUC	standard error	AUC	standard error
ROT_{TH}	0.830	0.04	0.855	0.05	0.809	0.05
$rROT_{TH}$	0.788	0.04	0.828	0.05	0.754	0.06
ROT_{HM}	0.739	0.05	0.759	0.06	0.721	0.06
$rROT_{HM}$	0.694	0.05	0.728	0.06	0.664	0.06
ROT_{HMUS}	0.871	0.04	0.876	0.04	0.867	0.04
$rROT_{HMUS}$	0.840	0.04	0.856	0.05	0.825	0.05
ROT_{US}	0.938	0.02	0.946	0.03	0.930	0.03
$rROT_{US}$	0.906	0.03	0.916	0.04	0.898	0.04

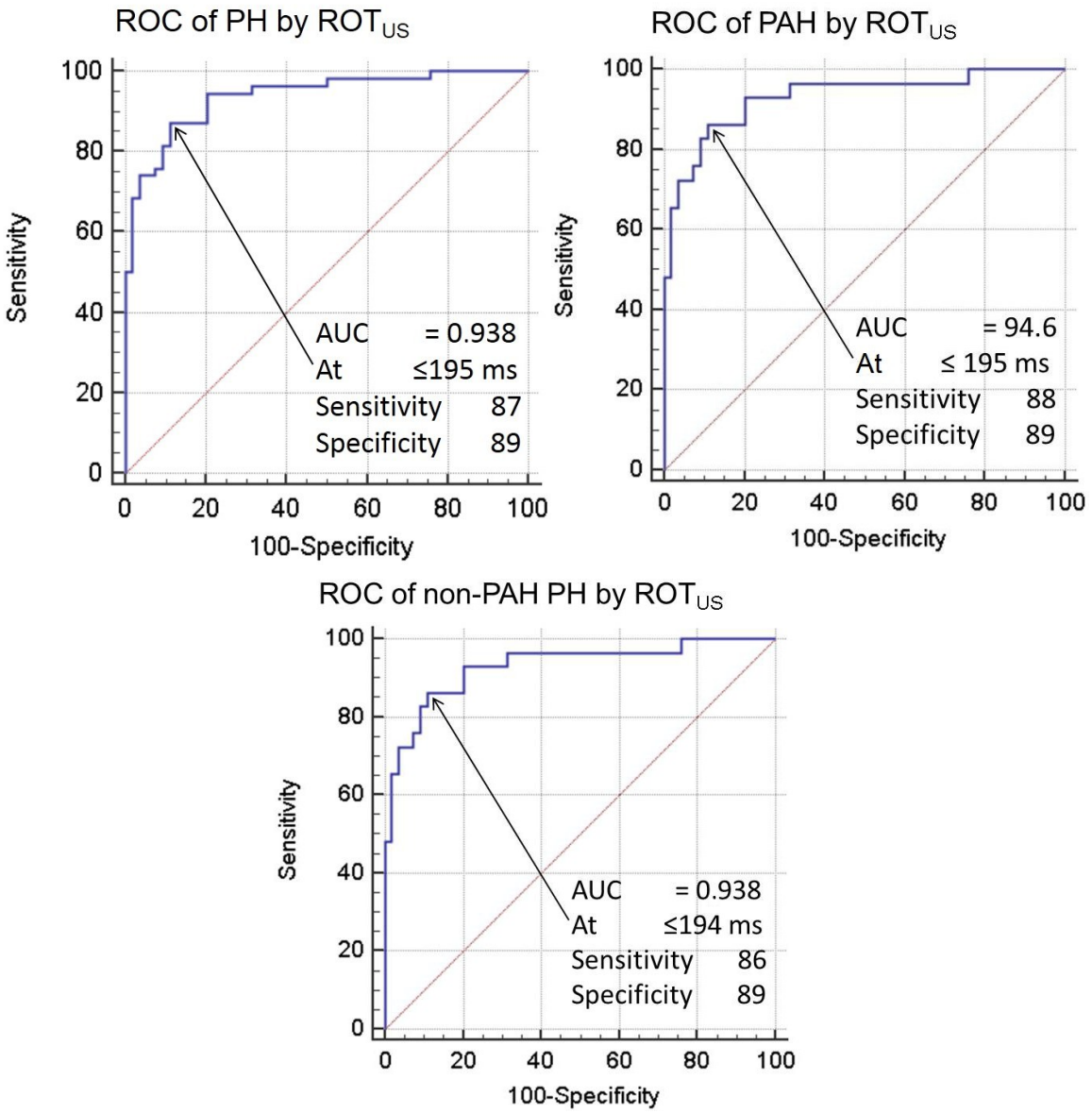

Figure 20: ROC curves for the diagnosis of PH employing ROT$_{US}$. Diagnostic performance of ROT$_{US}$ to diagnose PH within all patients (A), within PAH and non-PH patients (B), and within non-PAH PH and non-PH patients (C). AUC = area under the curve, PH = pulmonary hypertension, PAH = pulmonary arterial hypertension. Sensitivity and specificity are given in %.

Cut-off values for diagnosing PH from ROT were chosen after maximal sum of sensitivity and specificity. Results for ROT derived from threshold, half-maximum, linear extrapolation below half-maximum, and full upslope linear extrapolation algorithms are summarised in Table 8.

Table 8: ROT cut-off values for the diagnosis of PH. sens = sensitivity, spec = specificity, ROT = onset time of retrograde blood flow derived from threshold (TH), half-maximum (HM), linear extrapolation below half-maximum (HMUS), and full upslope linear extrapolation (US) algorithms, rROT = onset time of retrograde blood flow relative to the cardiac interval derived from the algorithms same as listed above, a.u. = arbitrary unit.

	PH			**PAH**			**non-PAH PH**		
	cut-off (ms)	sens	spec	cut-off (ms)	sens	spec	cut-off (ms)	sens	spec
ROT_{TH}	≤257	61	91	≤258	72	87	≤309	79	69
ROT_{HM}	≤202	44	94	≤202	48	94	≤190	41	94
ROT_{HMUS}	≤187	78	85	≤187	80	85	≤184	76	85
ROT_{US}	≤195	87	89	≤195	88	89	≤194	86	89
	PH			**PAH**			**non-PAH PH**		
	cut-off (a.u.)	sens	spec	cut-off (a.u.)	sens	spec	cut-off (a.u.)	sens.	spec
$rROT_{TH}$	≤0.25	50	93	≤0.30	76	78	≤0,38	86	56
$rROT_{HM}$	≤0.26	52	80	≤0.26	60	80	≤0,20	31	94
$rROT_{HMUS}$	≤0.18	65	90	≤0.17	72	96	≤0,22	72	81
$rROT_{US}$	≤0.19	76	93	≤0.18	80	94	≤0,24	90	76

4 Discussion

ROT of blood flow in the MPA is significantly shortened in PAH, and moreover, in the other clinical PH groups. Employing upslope linear extrapolation of MPA and retrograde blood flow curves to determine ROT from evaluation of 2D through-plane MR-PCI of the MPA by routine clinical software, a cut-off value of $ROT_{US} \leq 195$ ms allowed the diagnosis of PH with a sensitivity of 87% and a specificity of 89%. Restricting the study population to PAH and non-PH subjects, the same cut-off allowed discrimination of PAH patients with 88%/89% sensitivity/specificity. Since non-PAH PH subjects also could be identified within patients with normal mPAP by a cut-off $ROT_{US} \leq 194$ ms with a sensitivity of 86% and a specificity of 89%, early ROT of blood flow in the MPA is not only a diagnostic index for patients with PAH, but also PH in general.

ECG-gated 2D through-plane MR-PCI enables the assessment of blood velocity and vessel area cross-section throughout the cardiac cycle. Data provide information on peak and average velocities, forwards and backwards blood flow, as well as net forwards blood volume (= stroke volume) in order to estimate cardiac output from stroke volume and heart rate. MR-PCI data of the ascending aorta and MPA are typically acquired and evaluated in routine cardiac MRI investigations. (25,26)

Besides routine evaluations, MR-PCI provides the assessment of various interesting non-invasive indices related to cardiovascular and right heart hemodynamic. Alterations in blood flow velocity fields in the MPA assessed by MR-PCI in patients with PH have been observed in numerous studies. Kondo et al. were the first who employed 2D through-plane encoded MR-PCI in the MPA to assess MPA blood flow in PH and reported the presence of an abnormal systolic retrograde blood flow in the MPA, which has been observed also in echocardiographic studies.(27)

Besides the retrograde flow, they documented lower systolic MPA peak velocity, larger MPA cross-section area, and reduced MPA vessel pulsatility in PH compared to normal subjects. These findings where further investigated by various authors, and related to pulmonary pressures. Sanz et al. found, that in PAH average MPA velocity is highly correlated with mPAP and sPAP ($r = -0.73$ and -0.76, $p<0.001$). By using a cut-off value for the average MPA velocity of 11.7 cm/sec, they were able to diagnose PAH with a sensitivity/specificity of 93%/82%.(20)

Strong correlations were also found between MPA cross-section areas and mPAP, predicting the presence of PH with 93% sensitivity and 63% specificity.(28) Similar alterations in MPA cross-section area and blood velocities were reported also in CTEPH.(29,30)

In the present study, the MPA cross-section was also found to be significantly larger in PH than non-PH patients ($p<0.0001$) and did not significantly differ between the PAH and non-PAH PH groups ($p=0.5983$, 0.5435 and 0.6790 for average, minimal and maximal MPA area, respectively). In line with the above mentioned studies, MPA cross-section area in the present study correlated positively with mPAP ($r = 0.64$), even though our PH patients were heterogeneous with respect to clinical groups. Mean velocity was, in accordance with literature, reduced in PH; however, correlation with mPAP was only moderate ($r = -0.49$). This result can be understood with respect to the fact that within different clinical PH groups of our study population alterations determining MPA velocity (e.g. reduced CO, decreased vascular compliance or left ventricular failure have major to minor influence) differ and therefore, the association of mean MPA velocity with mPAP is weakened.(8)

Since PH is a multifactorial, pathophysiological hemodynamic condition, non-invasive indices, which are not restricted to one specific clinical PH group, are of special interest for patient screening. Helderman et al. found that the early onset of retrograde blood flow in the MPA is a potential diagnostic index for PAH. In their study the authors showed that by choosing a cut-off of rROT at 0.25, PAH can be differentiated from non-PH patients.(23)

The onset time of this retrograde flow is determined by the existence of a PH-associated vortical blood flow in the MPA, which does not exist in patients with normal mPAP. From period of existence of vortical blood flow in the cardiac interval, mPAP can be estimated with physical accuracy ($R^2 = 0.95$), irrespectively of the aetiology of PH (97%/96% sensitivity/specificity for a cut-off value ≥ 14.3% of period of existence of vortical blood flow).(22,31)

In the above studies, authors used dedicated software and non-routine MR-PCI protocols, which limit the use of these indices in clinical routine. In the present study we were able to show that retrograde blood flow in the MPA can be evaluated from routine 2D through-plane MR-PCI series of the MPA by using standard ARGUS

FLOW software and manually outlining the region of retrograde flow within the MPA vessel cross-section throughout the cardiac cycle.(23,31)

To determine ROT from retrograde flow-time curves, various approaches are possible. Onset of flow can be for example determined from thresholds so that a rise in flow is taken as indicator. This technique can easily be automated, but noise or valvular flow can hamper correct assignment of onset times by a predefined threshold (Figure 21). If the thresholds were set too high, the blood flow onset time would be overestimated. Therefore, an algorithm based only on the definition of threshold would be rather prone to over- or underestimate the onset of blood flow within the cardiac interval.

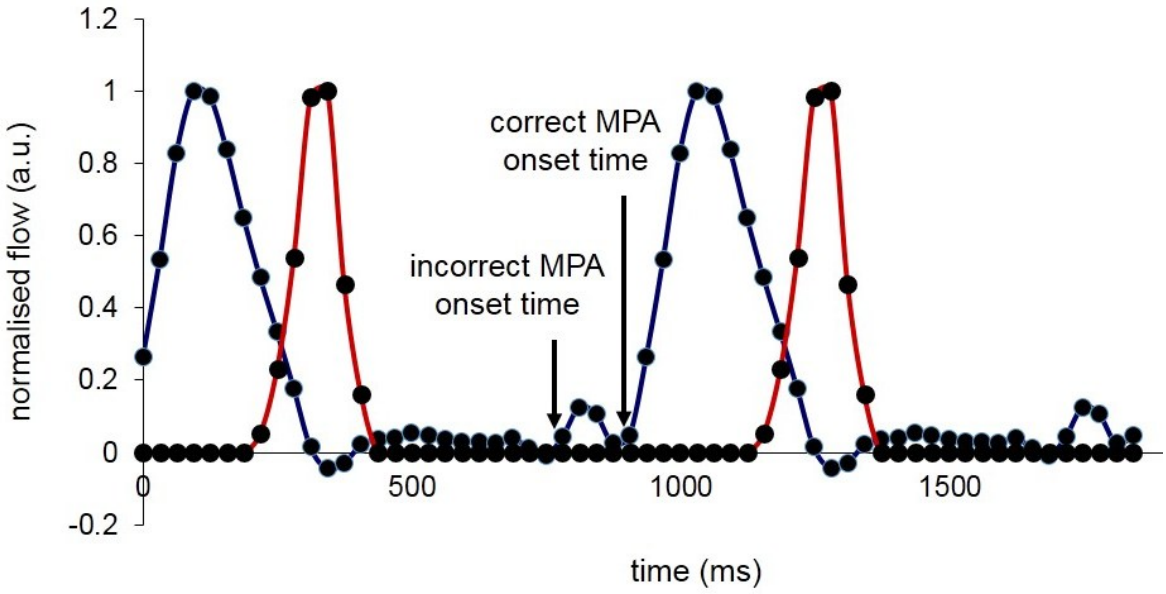

Figure 21: Limitation in calculation of ROT by the threshold algorithm. Definition of low thresholds leads to wrong definition of onset time of flow in the main pulmonary artery. a.u. = arbitrary unit.

The two algorithms half-maximum and half-maximum upslope fit were found to be inappropriate for the evaluation of ROT, since blood flow curves sometimes revealed only one flow value between 0 and the half-maximum (Figure 22). This was due to the rather low MR-PCI time resolution (repetition time = 77 ms) in the present study, which was to keep breath-hold periods during image acquisition reasonably short (19 heart beats). Since these two algorithms need at least 2 data points to calculate a line, the two last points before half maximum were used, which caused

an underestimation of the ROTs (Figure 22). It can be assumed that with higher time resolution in MR-PCI data, the half-maximum evaluation of ROT provides automatic assessment of MPA forward and retrospective blood flow onset times.

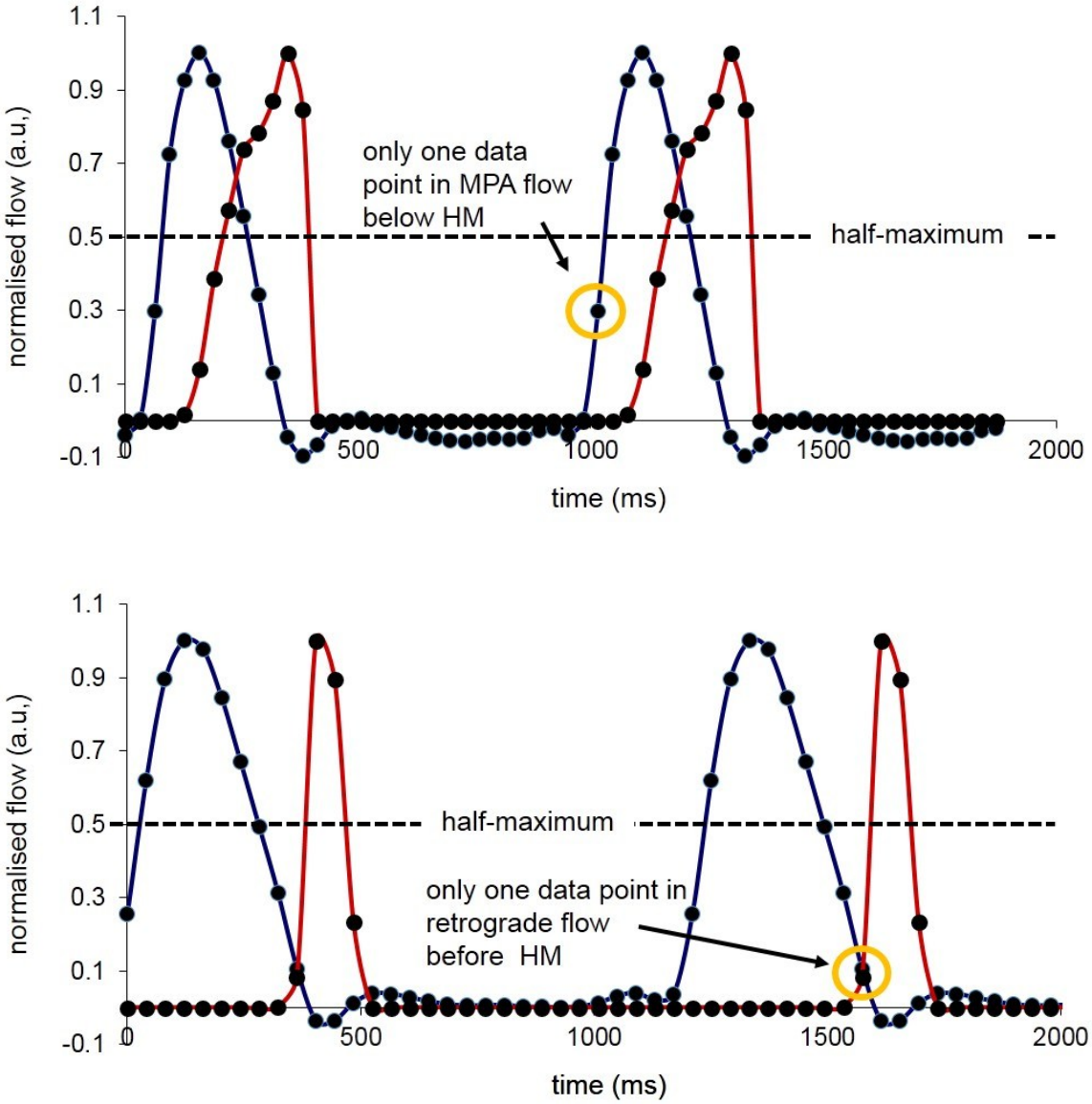

Figure 22: Half-maximum and half-maximum upslope fit analysis. Fits could not be performed if less than two flow data points were measured before the half-maximum is reached. Examples of failing of half-maximum analysis in the main pulmonary artery (upper graph) and in retrograde flow (lower graph). The blue line represents measured MPA flow (ROI 1), red line retrograde flow (ROI 2) respectively. a.u. = arbitrary unit.

In our study it was possible to calculate the ROTs of the forward and retrograde flows in the MPA with full upslope linear extrapolation in all cases without specific

problems. This method however needs manual input to define which data points should be used for the fit and linear extrapolation of flow curves.

According to the results of the ROC curve analysis, the highest AUC were achieved from ROTs determined by full upslope linear extrapolation of flow curves. Therefore, we assume this technique as the most reliable to determine ROC from respective MR-PCI data. In line with the cut-off value for diagnosis of PAH from ROT = 185 ms reported by Helderman et al., we found an optimal cut-off at a $ROT_{US} \leq$ 195 ms for diagnosis of PH and PAH (87%/89% sensitivity/specificity and 88%/89%, sensitivity/specificity, respectively)(23)

The cut-off for non-PAH PH at a $ROT_{US} \leq 194$ ms diagnosed PH with a sensitivity and specificity of 86% and 89%. The $ROT_{US} \leq 195$ ms suggests that early ROT flow in the MPA is not only a diagnostic marker for PAH, but also for PH in general. In accordance with Helderman et al., ROT and rROT were negatively correlated with mPAP ($r = -0.67$). The correlation of ROT with mPAP found in our heterogeneous study population was however, much weaker than in the study by Helderman et al ($R^2 = 0.62$). This difference might be explained by two major limitations in our study:

As we retrospectively evaluated MR-PCI of the main pulmonary artery, image positions and orientations were not always optimal. Sometimes imaging planes were located too close to the pulmonary valve (Figure 4A), resulting in MPA flow patterns determined by valvular vortices, which were difficult to exclude from retrograde blood flow. In case the MR-PCI position was close to the pulmonary artery bifurcation, in-plane motion of blood into the left/right pulmonary branches tampered with MPA through-plane velocities. Secondly, the background phases could not be corrected by the software. As the background phases vary in space but not within the cardiac interval, it could be assumed, that background drifts should not have a major impact on the timing of early ROT.(32–34)

5 Conclusion and Clinical Relevance

In conclusion, the results of the present study show that ROT of blood flow in the MPA can be evaluated from routine 2D through-plane velocity encoded MR-PCI of the MPA by standard ARGUS FLOW software. Even though ROT of blood flow in the MPA did not allow accurate estimations of mPAP, the results of this study indicate that early ROT represent a reliable, non-invasive index for the diagnosis of not only PAH, but also PH in general. As 2D through-plane velocity encoded MR-PCI of the MPA is included in numerous clinical routine protocols, ROT could be evaluated easily, enabling PH screening in patients undergoing cardiac magnetic resonance investigations.

6 Bibliography

1. Kroegel C, Bonella F. Klinische Pneumologie das Referenzwerk für Klinik und Praxis. 1st ed. Stuttgart a.o.: Thieme; 2014.

2. Hoeper MM, Bogaard HJ, Condliffe R, Frantz R, Khanna D, Kurzyna M, et al. Definitions and diagnosis of pulmonary hypertension. J Am Coll Cardiol 2013;62(25 Suppl):D42-50.

3. Kovacs G, Berghold A, Scheidl S, Olschewski H. Pulmonary arterial pressure during rest and exercise in healthy subjects: a systematic review. Eur Respir J 2009;34(4):888-894.

4. Galiè N, Humbert M, Vachiery J, Gibbs S, Lang I, Torbicki A, et al. 2015 ESC/ERS Guidelines for the diagnosis and treatment of pulmonary hypertension. Eur Heart J 2015 The Oxford University Press.

5. Bradlow WM, Gibbs JS, Mohiaddin RH. Cardiovascular magnetic resonance in pulmonary hypertension. J Cardiovasc Magn Reson 2012;14:6-429X-14-6.

6. Humbert M, Gerry Coghlan J, Khanna D. Early detection and management of pulmonary arterial hypertension. Eur Respir Rev 2012;21(126):306-312.

7. Badesch DB, Champion HC, Sanchez MA, Hoeper MM, Loyd JE, Manes A, et al. Diagnosis and assessment of pulmonary arterial hypertension. J Am Coll Cardiol 2009;54(1 Suppl):S55-66.

8. Simonneau G, Gatzoulis MA, Adatia I, Celermajer D, Denton C, Ghofrani A, et al. Updated clinical classification of pulmonary hypertension. J Am Coll Cardiol 2013;62(25 Suppl):D34-41.

9. Oudiz RJ. Pulmonary hypertension associated with left-sided heart disease. Clin Chest Med 2007;28(1):233-41, x.

10. Tapson VF, Humbert M. Incidence and prevalence of chronic thromboembolic pulmonary hypertension: from acute to chronic pulmonary embolism. Proc Am Thorac Soc 2006;3(7):564-567.

11. Pengo V, Lensing AW, Prins MH, Marchiori A, Davidson BL, Tiozzo F, et al. Incidence of chronic thromboembolic pulmonary hypertension after pulmonary embolism. N Engl J Med 2004;350(22):2257-2264.

12. dos Santos Fernandes CJ, Jardim CV, Hovnanian A, Hoette S, Dias BA, Souza S, et al. Survival in schistosomiasis-associated pulmonary arterial hypertension. J Am Coll Cardiol 2010;56(9):715-720.

13. Stouffer GA. Cardiovascular Hemodynamics for the Clinician. Malden, Massachusetts: Blackwell Futura; 2008.

14. Hien P. Praktische Pneumologie mit einer Vielzahl von Übersichten. Berlin a.o.: Springer; 2012. Available from: http://dx.doi.org/10.1007/978-3-642-10209-7

15. Marini JJ, Wheeler AP. Critical Care Medicine : The Essentials. 4th ed. Philadelphia: Wolters Kluwer Lippincott Williams & Wilkins; 2009.

16. Hoeper MM, Lee SH, Voswinckel R, Palazzini M, Jais X, Marinelli A, et al. Complications of Right Heart Catheterization Procedures in Patients With Pulmonary Hypertension in Experienced Centers. J Am Coll Cardiol 2006;48(12):2546-2552.

17. Kovacs G, Reiter G, Reiter U, Rienmuller R, Peacock A, Olschewski H. The emerging role of magnetic resonance imaging in the diagnosis and management of pulmonary hypertension. Respiration 2008;76(4):458-470.

18. Mackey ES, Sandler MP, Campbell RM, Graham TP,Jr, Atkinson JB, Price R, et al. Right ventricular myocardial mass quantification with magnetic resonance imaging. Am J Cardiol 1990;65(7):529-532.

19. Boxt LM, Katz J. Magnetic resonance imaging for quantitation of right ventricular volume in patients with pulmonary hypertension. J Thorac Imaging 1993;8(2):92-97.

20. Sanz J, Kuschnir P, Rius T, Salguero R, Sulica R, Einstein AJ, et al. Pulmonary arterial hypertension: noninvasive detection with phase-contrast MR imaging. Radiology 2007;243(1):70-79.

21. Peng H, Chung H, Yu H, Tseng WI. Estimation of pulse wave velocity in main pulmonary artery with phase contrast MRI: Preliminary investigation. Journal of Magnetic Resonance Imaging 2006;24(6):1303-1310.

22. Reiter G, Reiter U, Kovacs G, Kainz B, Schmidt K, Maier R, et al. Magnetic resonance-derived 3-dimensional blood flow patterns in the main pulmonary artery as a marker of pulmonary hypertension and a measure of elevated mean pulmonary arterial pressure. Circ Cardiovasc Imaging 2008;1(1):23-30.

23. Helderman F, Mauritz GJ, Andringa KE, Vonk-Noordegraaf A, Marcus JT. Early onset of retrograde flow in the main pulmonary artery is a characteristic of pulmonary arterial hypertension. J Magn Reson Imaging 2011;33(6):1362-1368.

24. Mosteller RD. Simplified calculation of body-surface area. N Engl J Med 1987;317(17):1098.

25. Schulz-Menger J, Bluemke DA, Bremerich J, Flamm SD, Fogel MA, Friedrich MG, et al. Standardized image interpretation and post processing in cardiovascular magnetic resonance: Society for Cardiovascular Magnetic Resonance (SCMR) board of trustees task force on standardized post processing. J Cardiovasc Magn Reson 2013;15:35-429X-15-35.

26. Hundley W, Bluemke DA, Finn J, et al. ACCF/ACR/AHA/NASCI/SCMR 2010 Expert Consensus Document on Cardiovascular Magnetic Resonance: A Report of the American College of Cardiology Foundation Task Force on Expert Consensus Documents. J Am Coll Cardiol. 2010;55(23):2614-2662.

27. Kondo C, Caputo GR, Masui T, Foster E, O'Sullivan M, Stulbarg MS, et al. Pulmonary hypertension: pulmonary flow quantification and flow profile analysis with velocity-encoded cine MR imaging. Radiology 1992; 183(3):751-758.

28. Sanz J, Kariisa M, Dellegrottaglie S, Prat-González S, Garcia MJ, Fuster V, et al. Evaluation of Pulmonary Artery Stiffness in Pulmonary Hypertension With Cardiac Magnetic Resonance. JACC: Cardiovascular Imaging 2009;2(3):286-295.

29. Kreitner KF, Kunz RP, Ley S, Oberholzer K, Neeb D, Gast KK, et al. Chronic thromboembolic pulmonary hypertension - assessment by magnetic resonance imaging. Eur Radiol 2007;17(1):11-21.

30. Ley S, Ley-Zaporozhan J, Pitton MB, Schneider J, Wirth GM, Mayer E, et al. Diagnostic performance of state-of-the-art imaging techniques for morphological

assessment of vascular abnormalities in patients with chronic thromboembolic pulmonary hypertension (CTEPH). Eur Radiol 2012;22(3):607-616.

31. Reiter G, Reiter U, Kovacs G, Olschewski H, Fuchsjager M. Blood flow vortices along the main pulmonary artery measured with MR imaging for diagnosis of pulmonary hypertension. Radiology 2015;275(1):71-79.

32. Lankhaar JW, Hofman MB, Marcus JT, Zwanenburg JJ, Faes TJ, Vonk-Noordegraaf A. Correction of phase offset errors in main pulmonary artery flow quantification. J Magn Reson Imaging 2005;22(1):73-79.

33. Rigsby CK, Hilpipre N, McNeal GR, Zhang G, Boylan EE, Popescu AR, et al. Analysis of an automated background correction method for cardiovascular MR phase contrast imaging in children and young adults. Pediatr Radiol 2014;44(3):265-273.

34. Gatehouse PD, Rolf MP, Graves MJ, Hofman MB, Totman J, Werner B, et al. Flow measurement by cardiovascular magnetic resonance: a multi-centre multi-vendor study of background phase offset errors that can compromise the accuracy of derived regurgitant or shunt flow measurements. J Cardiovasc Magn Reson 2010;12:5-429X-12-5.